GPO PRICE $ _____

CFSTI PRICE(S) $ _____

Hard copy (HC) 3.00

Microfiche (MF) .65

ff 653 July 65

[redacted]

NASA TT F-8326

[redacted]

[redacted] and

PRELIMINARY INVESTIGATIONS CONCERNING THE HYPERSONIC GLIDER

by Ph. Poisson-Quinton, R. Ceresuela, and G. Bernet

N67 17872 (ACCESSION NUMBER) (THRU)

35 (PAGES) 1 (CODE)

(NASA CR OR TMX OR AD NUMBER) 09 (CATEGORY)

FACILITY FORM 602

NATIONAL AERONAUTICS AND SPACE ADMINISTRATION
WASHINGTON January 1963

FIFTH EUROPEAN AERONAUTICAL CONGRESS

VENICE, 12 to 15 September 1962.

PRELIMINARY INVESTIGATIONS CONCERNING THE HYPERSONIC GLIDER

by Ph. POISSON-QUINTON*
R. CERESUELA**
G. BERNET***

SUMMARY AND FIGURES

I. Within the framework of the experimental investigations /1
undertaken by the O.N.E.R.A. at its new hypersonic installations (Fig. 3: Gust wind tunnels, M=7 and 10, and an arch-shaped tunnel, M=17), the hypersonic glider constitutes an object of activity that makes it possible to approach the problems of lifting capacity, of fineness, and of longitudinal stability at very high flight speeds.

It is first called to mind (Fig. 1) that the hypersonic glider has a lift that is superior to a ballistic object only then - provided the same initial velocity has been imparted - when its fineness exceeds 2; almost the entire trajectory of a glider is described at hypersonic speeds, and it is important to measure, in an acceptable way, the fineness that can be realized within a range of Mach numbers extending from 20 to 5 (Fig. 2); unfortunately, the blunted shapes, which are required to limit the heating of the glider, are rather unfavorable as far as a high efficiency is concerned, and it is necessary to look for compromise solutions.

*Chief of the Research Division) at the Direction of Aerodynamics of
**Chief of the Research Group) the O.N.E.R.A.
at Chatillon-sous-Bagneux.
***Chief of Wind Tunnels, at the Direction of Aerodynamics of the
O.N.E.R.A. at Chalais-Meudon.

II. The Reynold numbers which were obtained during these tests, /1
are of the order of magnitude of one-third of those that are found during balanced flight for a glider having a length of 6 meters (Fig. 4); moreover, the experiments have demonstrated that the Reynolds number directly affects, in the hypersonic field, the increase of the drag that is connected with the phenomenon of "viscous interference"; an experimental comparison (Fig. 5) with results obtained at Tullahome (V.K.F.) by the use of a "standard" glider shows the importance of that parameter; /2
on the other hand, it is not yet possible to analyze it in an acceptable manner; the evolution of the aerodynamic factors of this glider is given between the Mach numbers of 2 and 10 and is confronted with the calculation that is made possible by Newton's theory (Fig. 6,7, and 8).

III. Beginning with a configuration of a "basic glider" (delta wing of 75°, fuselage above the wing so as to limit its heating to the incidences of gliding), we have investigated the effects of the thickness of the flat wing and of the sweep at the leading edge (Fig. 9).

The approximate calculation of the drag at an incidence of zero by Newton's method has been performed for the basic glider (Fig. 10) and for the various thicknesses (Fig. 18) and sweeps (Fig. 20); the experimental evolution of the drag as a function of e/l and of $\phi°$ agrees well with the theoretical anticipations.

Newton's calculation of the characteristics of lifting capacity and induced drag (taking into account the gradual disappearance of the fuselage above the wing) as functions of the incidence accounts for the experimental evolution as measured in the ARCH tunnel at 17 Mach, (Fig. 11), particularly for high incidences.

The aerodynamic properties of the basic glider (strioscopic pictures: Fig. 26) have been supplied for Mach numbers ranging from 0.5 to 17 (Fig. 12 to 15): the continuity of the results obtained will be noted during the transition from the classical supersonic state to the hypersonic one; also noted will be the relative importance of the bottom drag under moderate supersonic conditions and of the viscous interference under high hypersonic conditions.

The characteristics of lifting capacity and drag at very large flight incidences are important to know for the investigation of the first phase (high altitude braking) of a re-entry of a glider from space; the experimental results that were obtained at M=10 up to an incidence of 90° (Fig. 16) follow well the evolution as anticipated on the basis of Newton's simple theory.

Changes of the thickness of the wing bring about solely a decalage of the polars (3 thicknesses at M=10, Fig. 17) while stressing the sweep makes it possible to improve the fineness (3 sweeps at M=7, Fig. 19);

finally, the evolution of the minimum drag and of the fineness as functions of the Mach number (Fig. 20) shows that the effect of the thickness (2.35 and 4.7%) and of the wingsweep (75° and 80°) is being preserved throughout the entire area of high-speed flight. /2

III (sic!). Inasmuch as the lengthwise stability is concerned, the fact that the fuselage gradually disappears in the "shadow" of the wing as the incidence increases leads, in the hypersonic field, to essentially nonlinear curves, and the margin of stability to be considered is the one which exists near the maximum fineness where the effect of the fuselage has practically disappeared. In regard to the longitudinal balance, it appears that an adaptation of the plane of the wing yields a higher aerodynamic return than the downward turn of surfaces controlling the trailing edge: the experiments show that a remarkable "noseup" torque can be obtained in that way, either by folding the forepart of the wing plane (folded delta of 75°, compared here to the solution of a "low fuselage" at M=7: Fig. 23), or by circular cambering of the skeleton (gothic wing of 75°: Fig. 24); in the latter case, we have established the requirement of an evolution of the radius of the leading edge that is proportionate to the cosinus of the local sweep - that leads to a thin trailing edge which makes it possible to have a better degree of fineness at moderate speeds where the bottom drag becomes important; but it also leads to a considerable drag in the hypersonic field, due to the large diameter of the bow; the "gothic" form of the leading edge also permits a better fineness than the delta wing of the same thickness (flat wing) and of the same dart-like form (Fig. 22), but it evidently causes more heating near the bow because the sweep is weaker there. /3

IV. A preliminary investigation of the heating that occurs on the leading edge of a sweptback wing was undertaken at Mach=10 (Fig. 25) in order to bring the experimental methods and the methods of analysis up-to-date; the model (which represents the forepart of a delta wing of 75° with circular leading edge) comprises, locally, a thin coating equipped with thermocouples; the rise of the temperature during the short time when the model is introduced into the hot hypersonic jetstream, makes it possible to undertake the measurement of the flow by taking into account the lateral losses as estimated on the basis of the analysis of the temperature at both sides of the stopping point; finally, the flow measured at the nose-end of the leading edge seems to decrease in a linear manner as the sweep increases; for pronounced sweeps, however, the experimental development is close to that of $\cos^{3/2}\phi$.

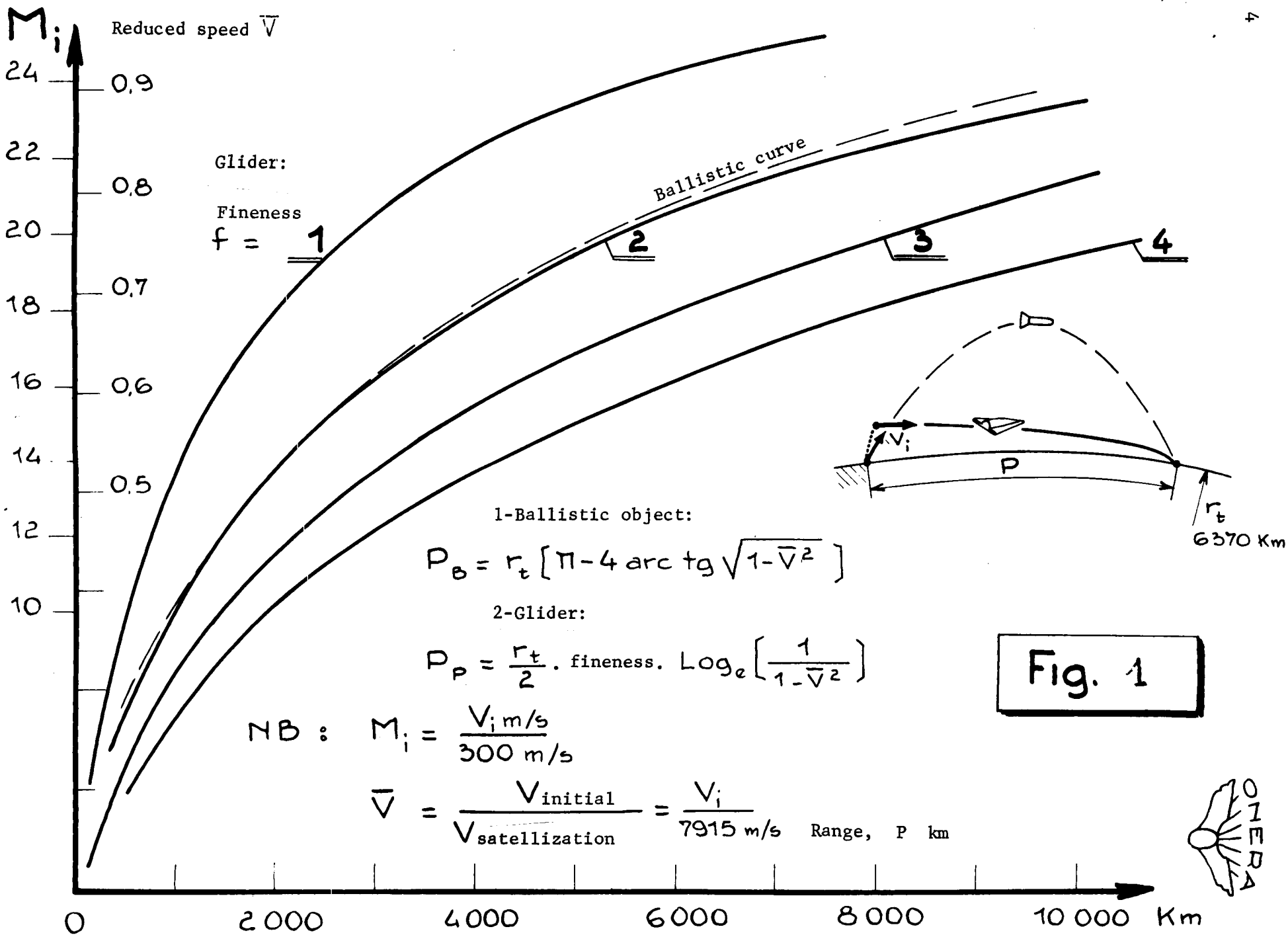
M_i
Reduced speed $\bar{V}$
24
22
20
18
16
14
12
10
0,9
0,8
0,7
0,6
0,5
Glider:
Fineness
f =
1
2
3
4
Ballistic curve
V_i
P
r_t
6370 Km
1-Ballistic object:
$P_B = r_t \left[\pi - 4 \text{ arc tg } \sqrt{1-\bar{V}^2} \right]$
2-Glider:
$P_P = \frac{r_t}{2} \cdot \text{fineness} \cdot \text{Log}_e \left[\frac{1}{1-\bar{V}^2} \right]$
NB : $M_i = \frac{V_i \text{ m/s}}{300 \text{ m/s}}$
$\bar{V} = \frac{V_{initial}}{V_{satellization}} = \frac{V_i}{7915 \text{ m/s}}$
Range, P km
0
2 000
4 000
6 000
8 000
10 000 Km

Fig. 1

Fig. 2

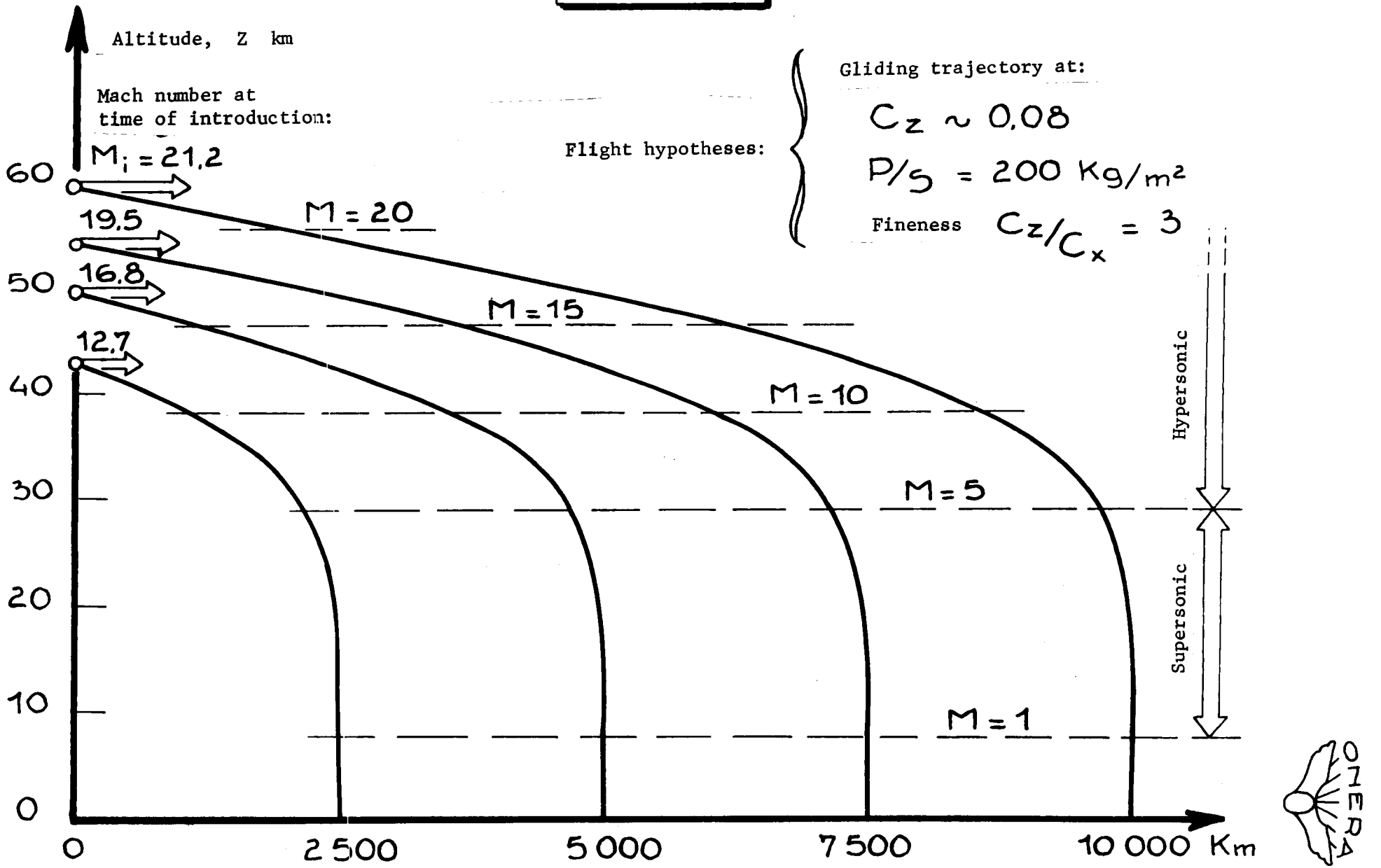

Range of the supersonic glider, in gliding flight

ONERA

Fig. 3

R2 Chalais M = 7

$25 < p_i < 75$ atm.
$T_i \sim 600°K$

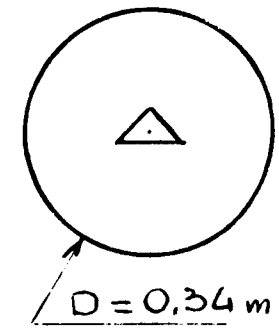

R'3 Chalais M ~ 10

$90 < p_i < 160$
$T_i \sim 1100°K$

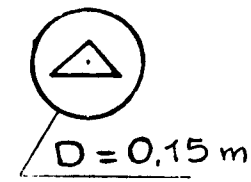

ARC1 Fontenay M ~ 17

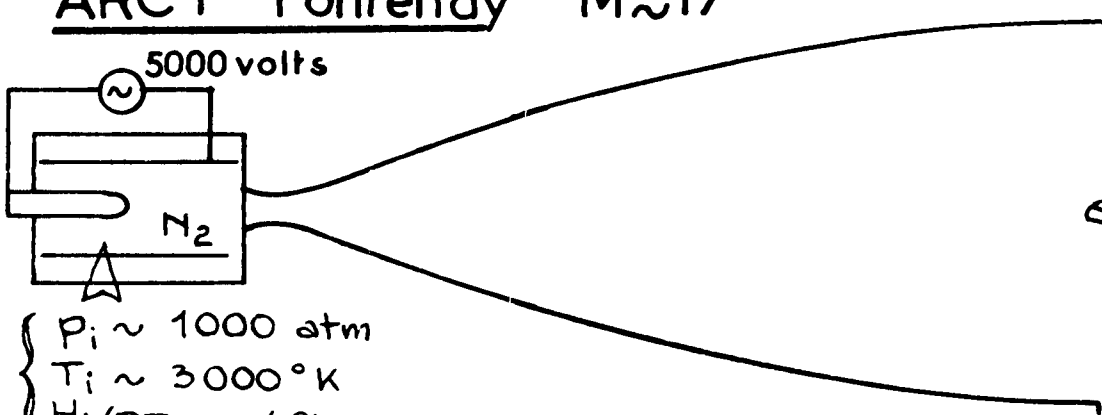

$P_i \sim 1000$ atm
$T_i \sim 3000°K$
$H_i/RT_a \sim 40$

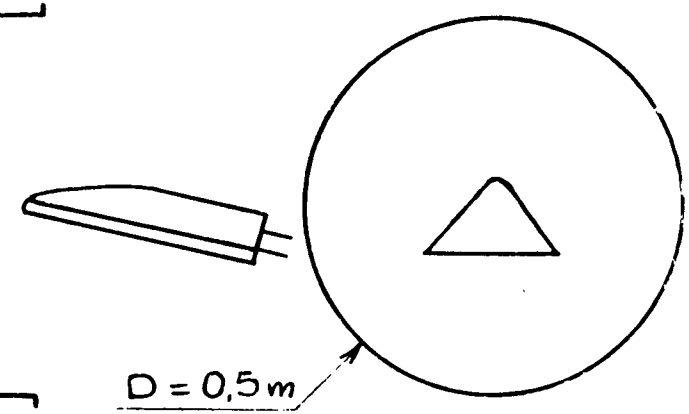

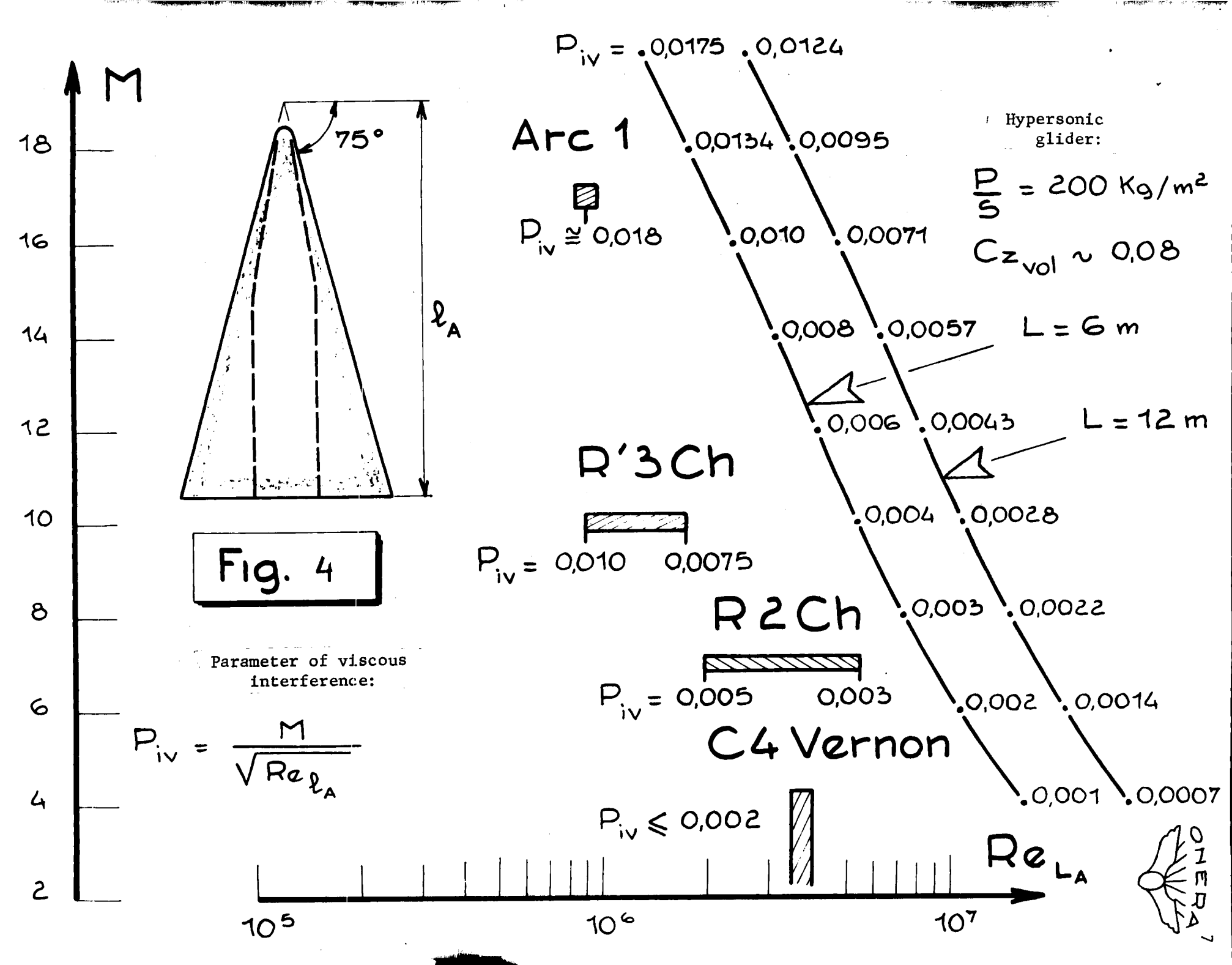
M
18
16
14
12
10
8
6
4
2
75°
ℓ_A
P_{iv} = 0,0175 0,0124
0,0134 0,0095
0,010 0,0071
0,008 0,0057
0,006 0,0043
0,004 0,0028
0,003 0,0022
0,002 0,0014
0,001 0,0007
Arc 1
$P_{iv} \cong 0{,}018$
R'3Ch
P_{iv} = 0,010 0,0075
R2Ch
P_{iv} = 0,005 0,003
C4 Vernon
$P_{iv} \leqslant 0{,}002$
Hypersonic glider:
$\frac{P}{S}$ = 200 Kg/m²
$C_{z_{vol}} \sim 0{,}08$
L = 6 m
L = 12 m
Re_{L_A}
10^5
10^6
10^7
Parameter of viscous interference:
$P_{iv} = \frac{M}{\sqrt{Re_{\ell_A}}}$
ONERA

Fig. 4

Fig. 5

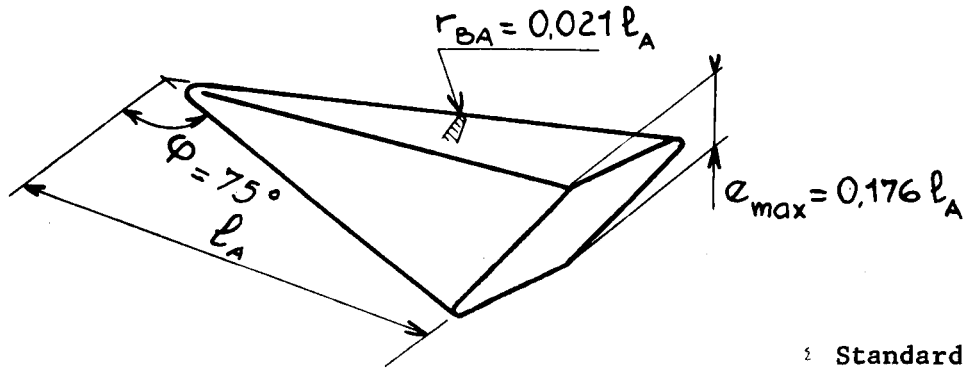

Standard glider

Total resistance

$C_{x_T}\ (i=0)$

ARC 1
16,2 > M > 14,6
$(T_P/T_i \sim 0{,}1)$

R'_3Ch
M ~ 10
$(T_P/T_i \sim 0{,}3)$

R_2Ch
M ~ 7
$(T_P/T_i \sim 0{,}5)$

Tullahoma :
VKF, M = 8
$(T_P/T_i \sim 0{,}8)$

VKF, M ≅ 20
$(T_P/T_i \sim 0{,}1)$

0,06
0,05
0,04
0,03
0,02
0,01

C_x value for $M/\sqrt{Re} \to 0$

Parameter of viscous interference $M/\sqrt{Re\, l_A}$

0,003 0,005 0,01 0,02 0,03 0,04 0,05

ONERA

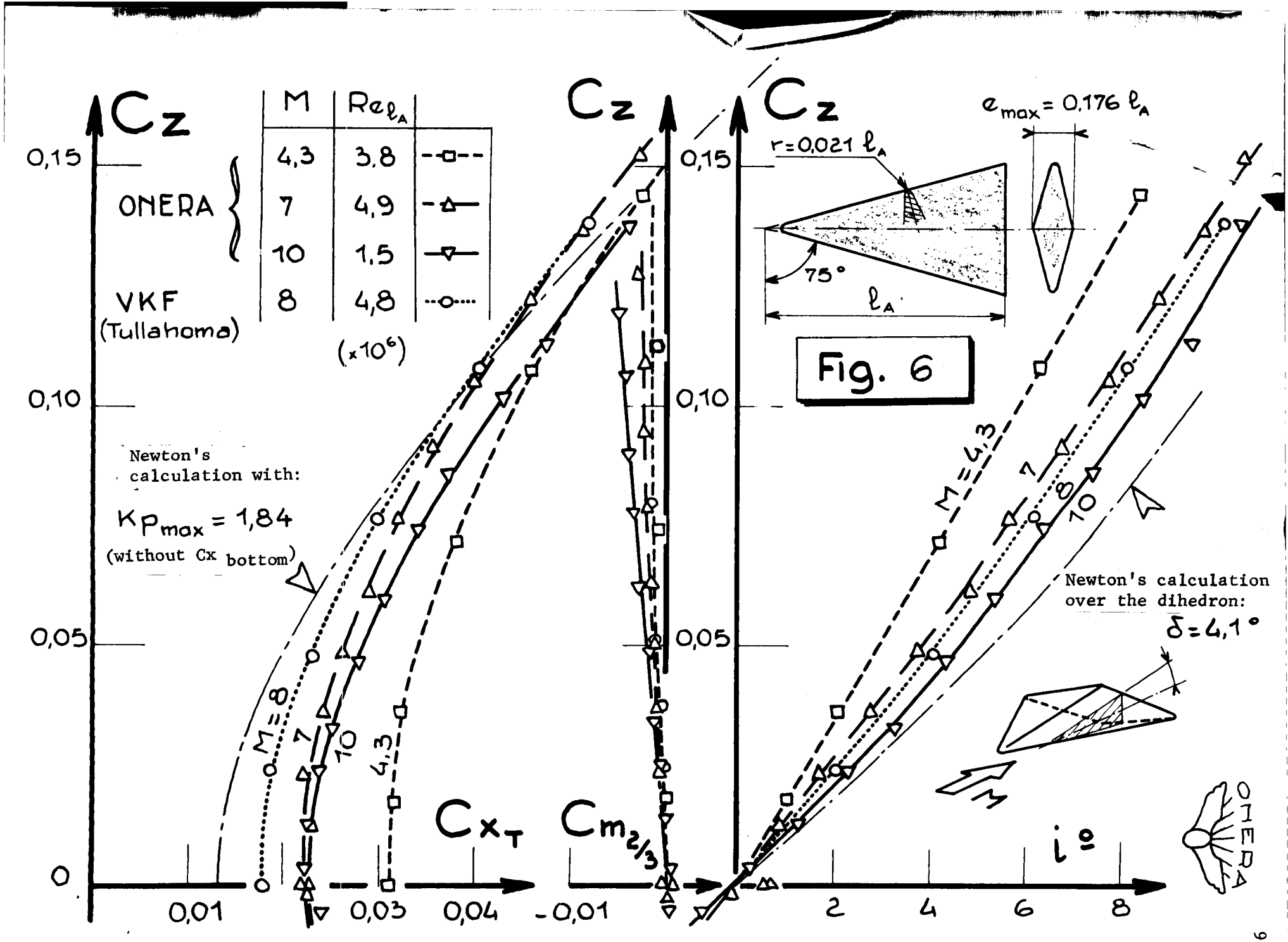
Cz
0,15
0,10
0,05
0
M
Re lA
ONERA
4,3
3,8
7
4,9
10
1,5
VKF
(Tullahoma)
8
4,8
(x10⁶)
Newton's
calculation with:
Kpmax = 1,84
(without Cx bottom)
M=8
7
10
4,3
Cxt
0,01
0,03
0,04
Cz
Cm2/3
-0,01
Cz
emax = 0,176 lA
r=0,021 lA
75°
lA
Fig. 6
0,15
0,10
0,05
M=4,3
7
8
10
Newton's calculation
over the dihedron:
δ=4,1°
M
i°
2
4
6
8
ONERA

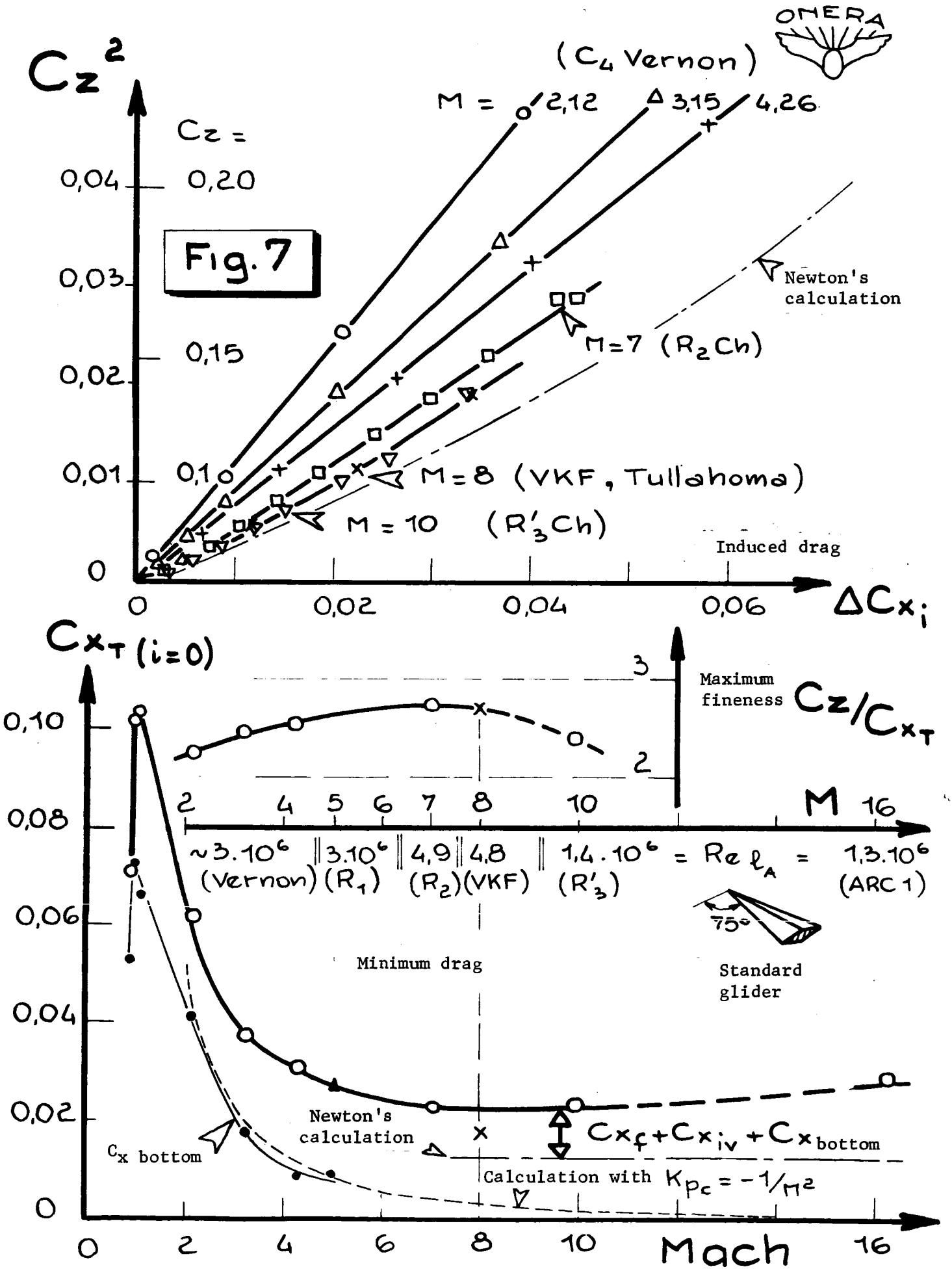
ONERA
C_z^2
(C_4 Vernon)
M = 2,12
3,15
4,26
Cz =
0,20
0,15
0,1
0,04
0,03
0,02
0,01
0
Fig. 7
Newton's calculation
M=7 (R_2Ch)
M=8 (VKF, Tullahoma)
M = 10 (R'_3Ch)
Induced drag
0
0,02
0,04
0,06
ΔC_{x_i}
C_{x_T} (i=0)
0,10
0,08
0,06
0,04
0,02
0
3
2
Maximum fineness C_z/C_{x_T}
2
4
5
6
7
8
10
M
16
~3.10⁶ (Vernon)
3.10⁶ (R_1)
4,9 4,8 (R_2)(VKF)
1,4.10⁶ (R'_3)
= Re ℓ_A =
1,3.10⁶ (ARC 1)
75°
Standard glider
Minimum drag
Newton's calculation
$C_{x_f}+C_{x_{iv}}+C_{x_{bottom}}$
$C_{x\ bottom}$
Calculation with $K_{p_c} = -1/M^2$
0
2
4
6
8
10
Mach
16

ONERA

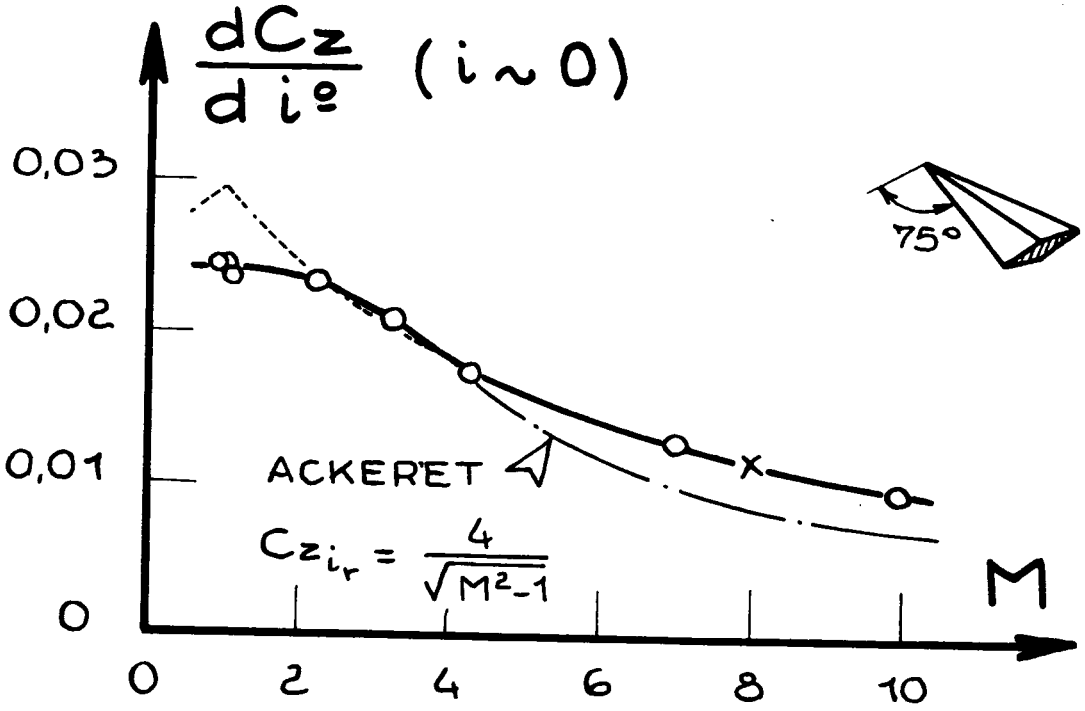
dCz/di° (i ~ 0)
0,03
0,02
0,01
0
75°
ACKERET
Cz_ir = 4/√(M²-1)
M
0
2
4
6
8
10

Fig. 8

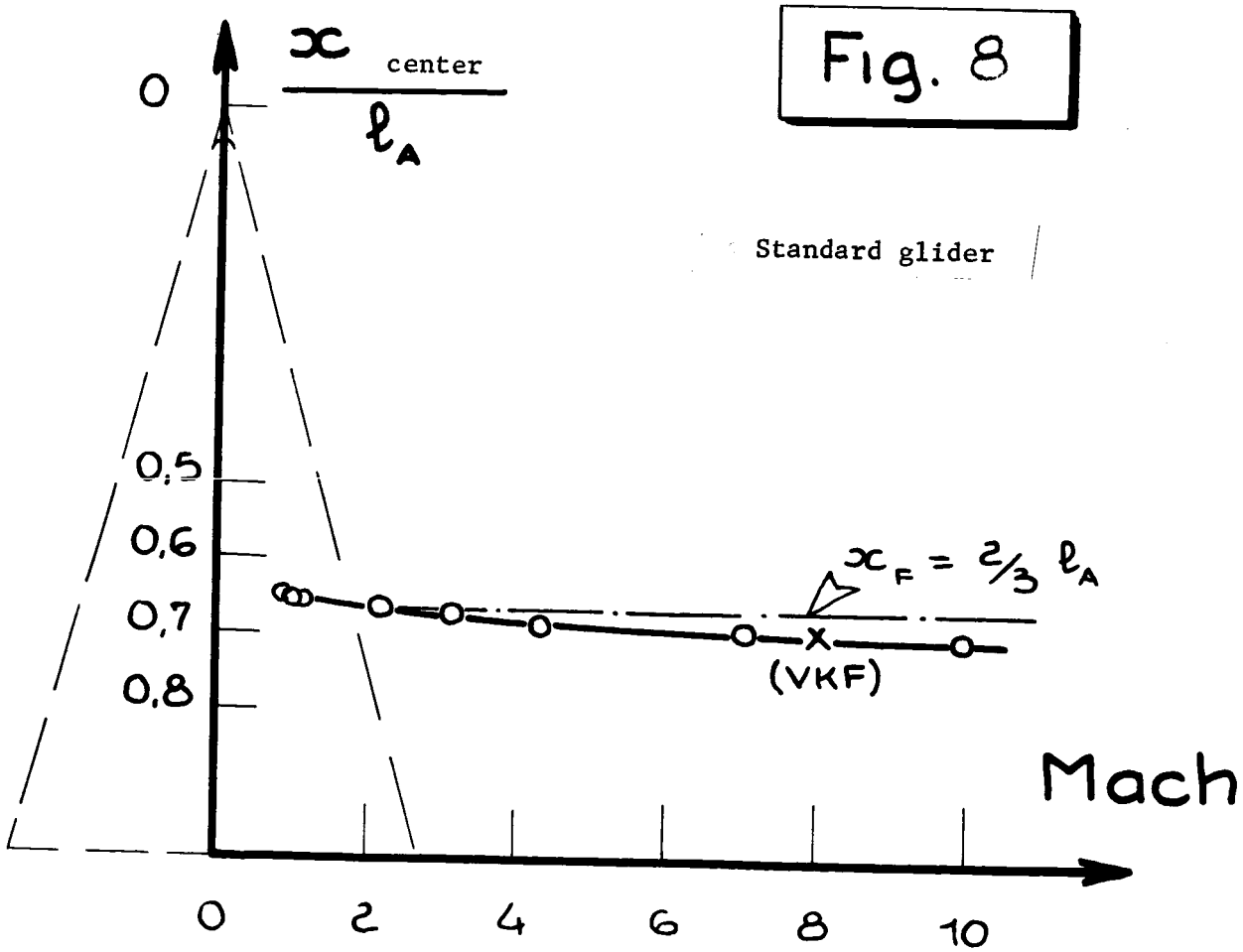
x center / l_A
0
0,5
0,6
0,7
0,8
Standard glider
x_F = 2/3 l_A
(VKF)
Mach
0
2
4
6
8
10

b. Effect of the sweep on $e = c^{te}$ and $S = c^{te}$.

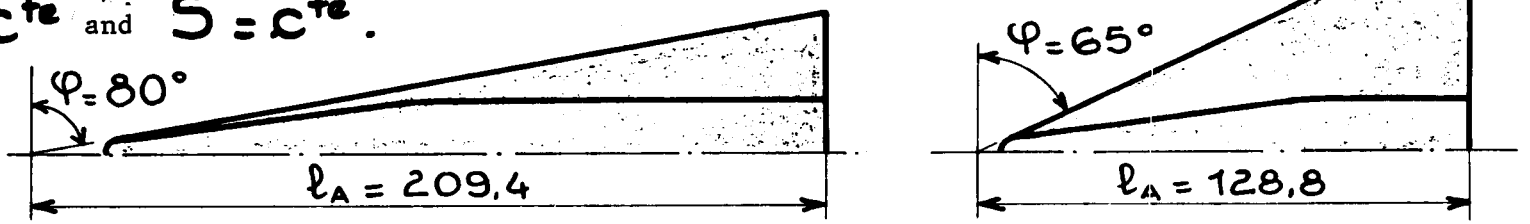

Basic glider

$\varphi = 75°$

$e/\ell_A = 2,35\%$

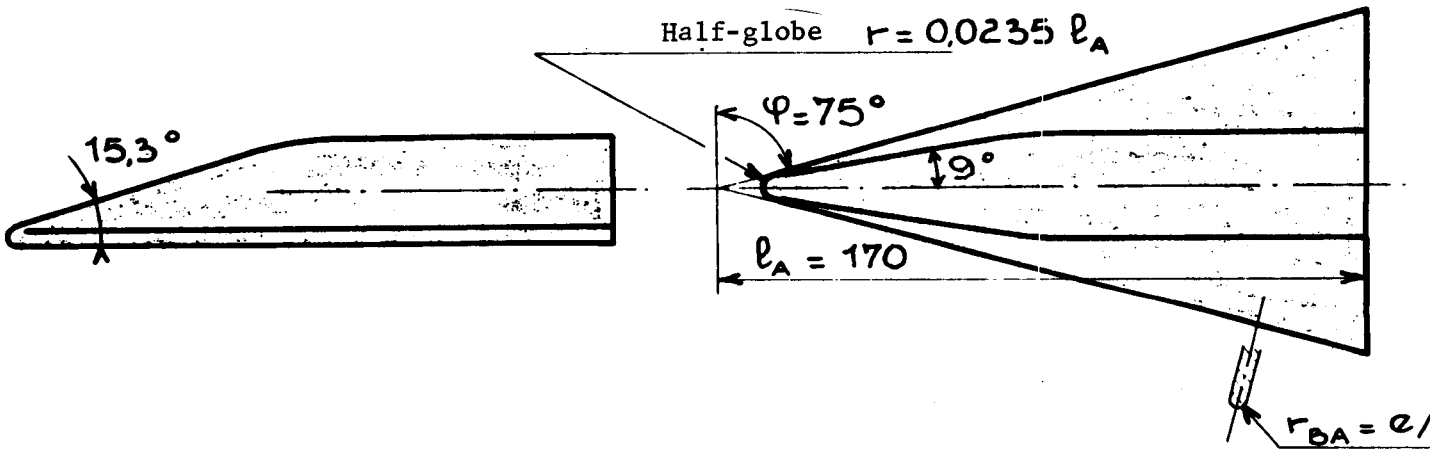

a. Effect of the thickness of the flat section in case of $\varphi = 75°$.

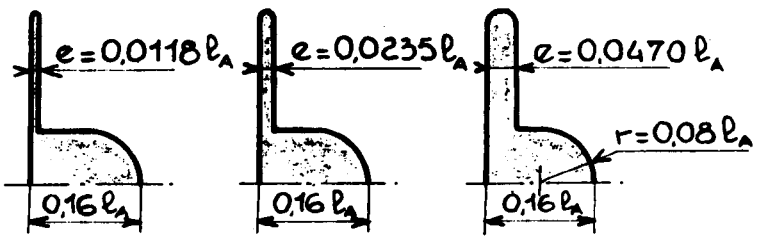

Fig. 9

Experimental investigation of a family of hypersonic gliders

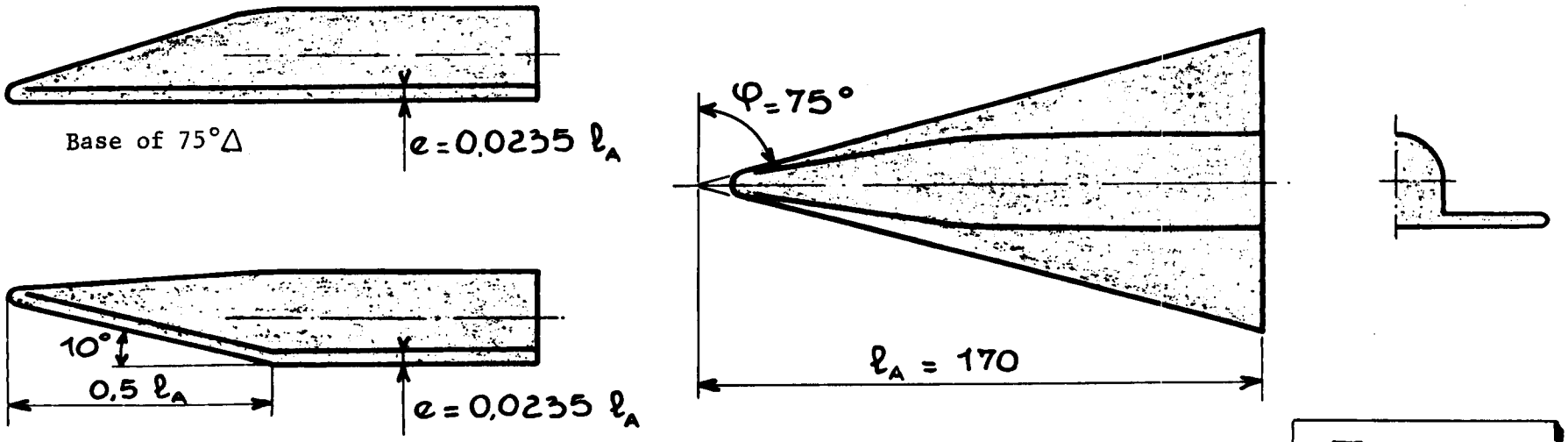

c. Folded skeleton 75°Δ

Fig. 9 bis

d. Flat wing, G75° e = 0.047 l_A

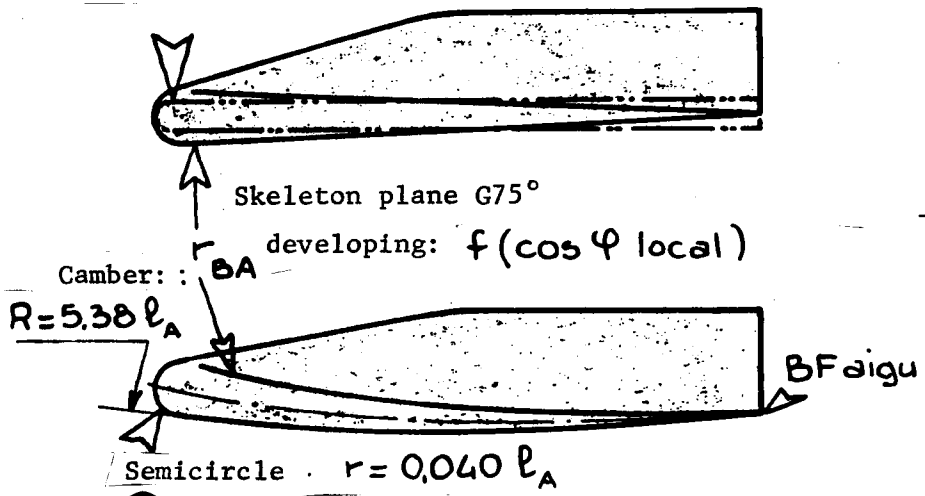

e. Cambered skeleton G75°

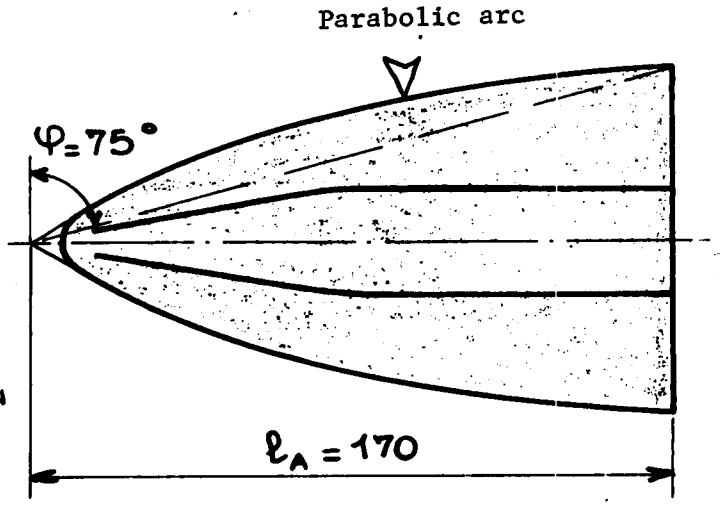

Gothic wings

(identical fuselage,

$S_G = 1,34\ S_\Delta$)

Hypersonic delta glider 75°

Calculated resistance C_{x_e}:

Fig.10

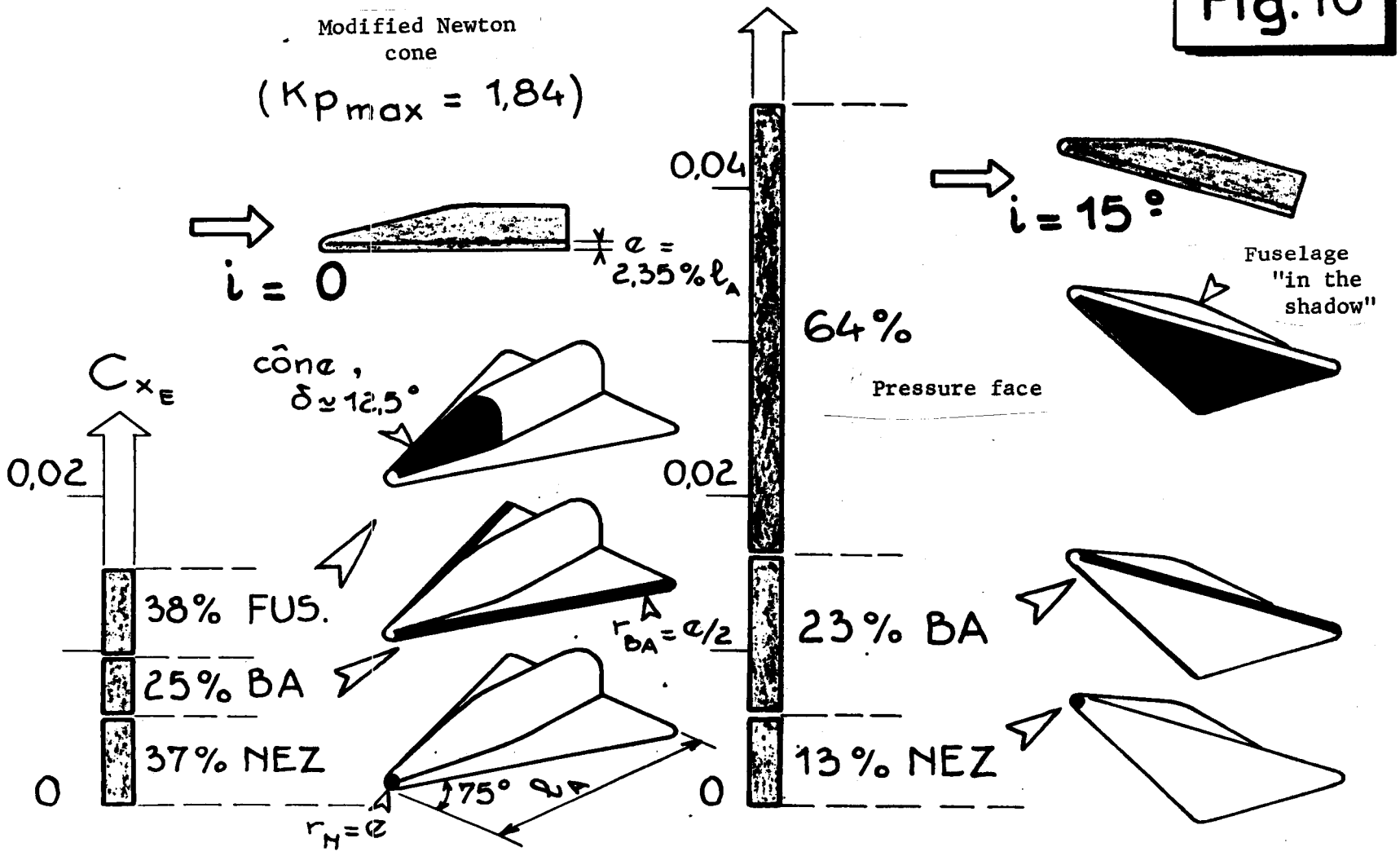

ONERA

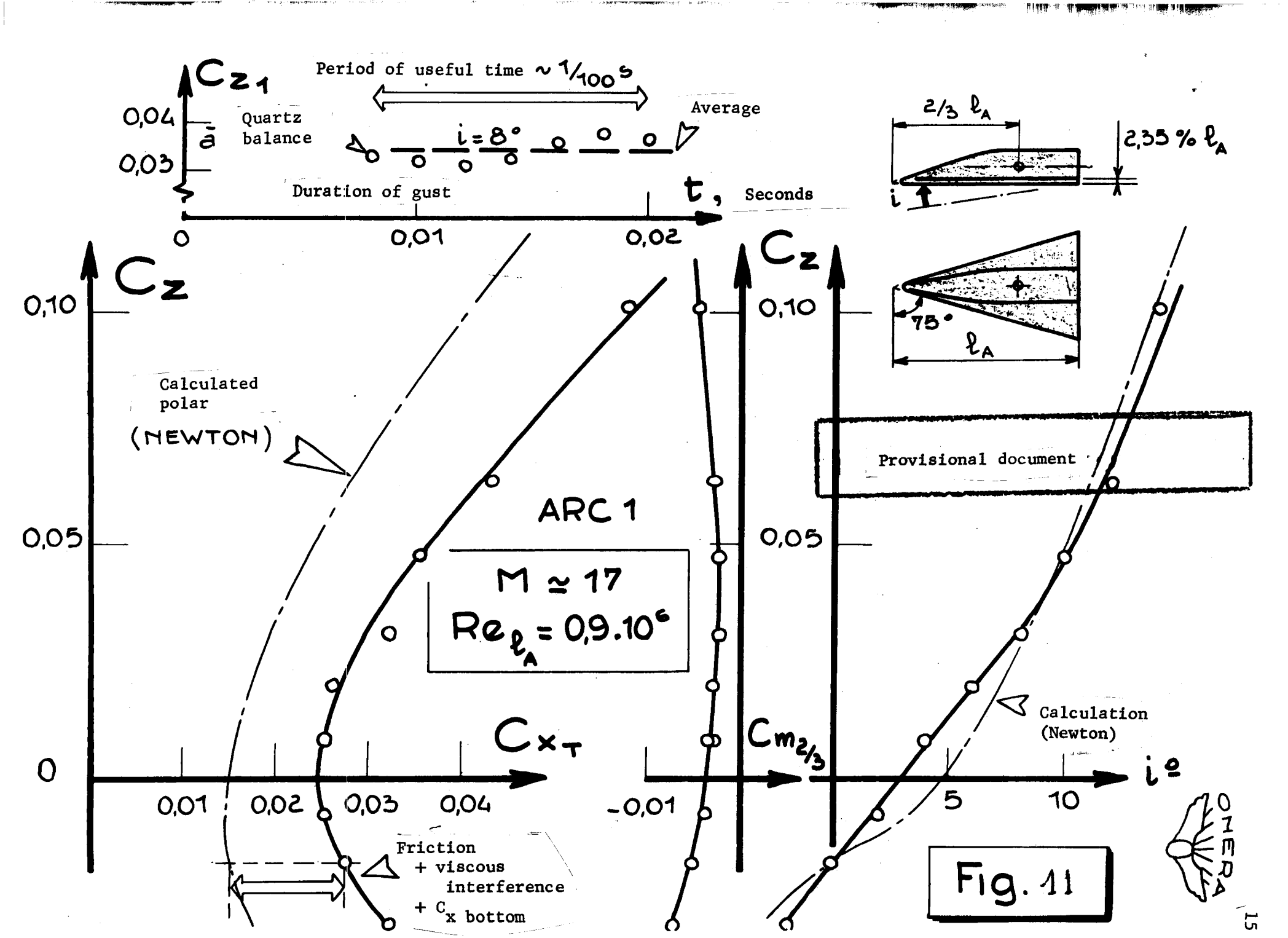
C_{z_1}
Period of useful time ~ 1/100 s
Average
0,04
0,03
$\bar{a}$
Quartz balance
i = 8°
Duration of gust
t, Seconds
0
0,01
0,02
2/3 ℓ_A
2,35 % ℓ_A
i
C_z
0,10
0,05
0
75°
ℓ_A
Calculated polar
(NEWTON)
Provisional document
ARC 1
M ≃ 17
$Re_{\ell_A} = 0{,}9.10^6$
C_{x_T}
0,01
0,02
0,03
0,04
Friction
+ viscous interference
+ C_x bottom
$C_{m_{2/3}}$
-0,01
5
10
i°
Calculation (Newton)
ONERA

Fig. 11

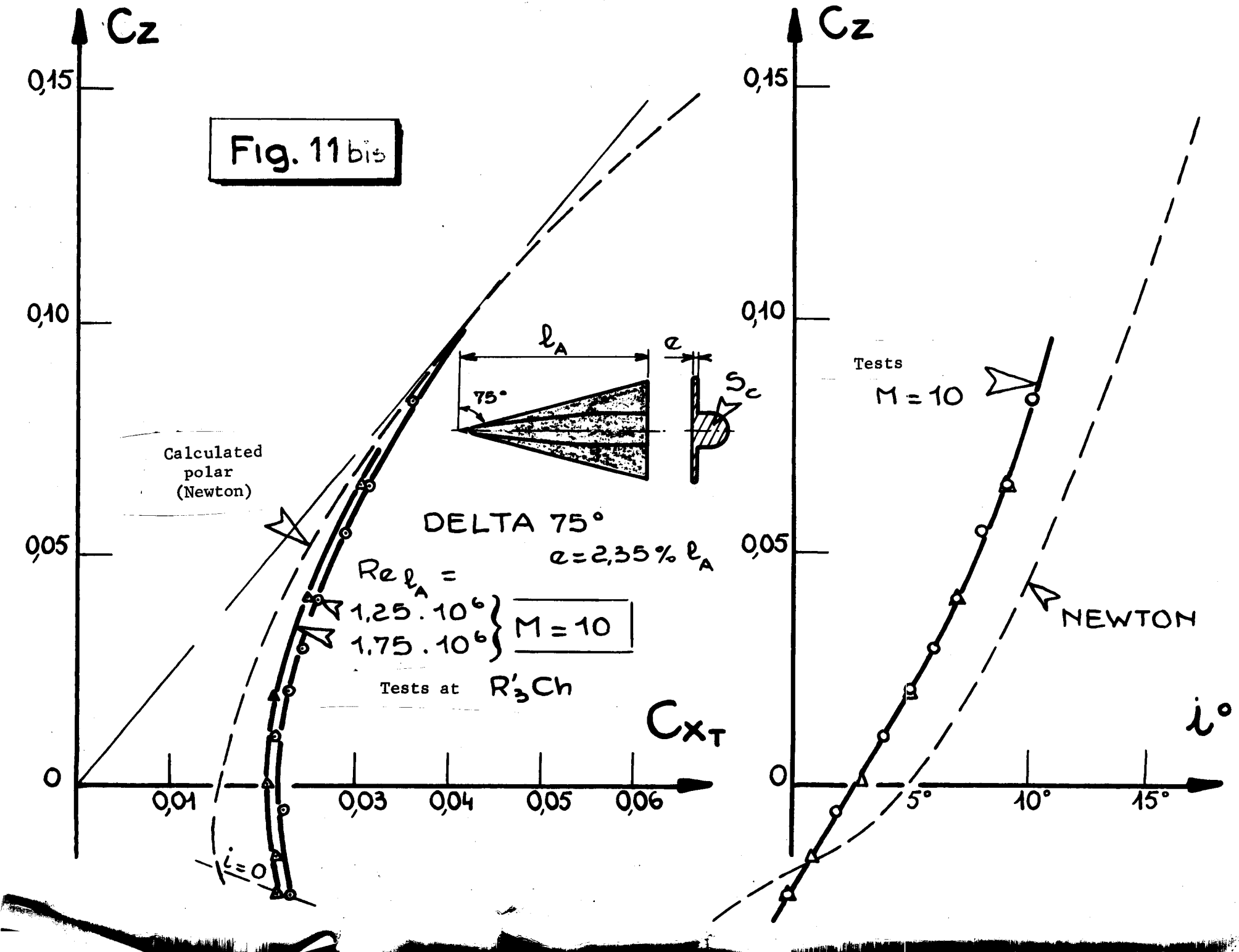
Fig. 11 bis
Cz
0,15
0,10
0,05
0
0,01
0,03
0,04
0,05
0,06
C_{X_T}
ℓ_A
e
75°
S_c
Calculated polar (Newton)
DELTA 75°
e = 2,35 % ℓ_A
Re_{ℓ_A} =
1,25 . 10⁶
1,75 . 10⁶
M = 10
Tests at R'_3Ch
i = 0
Cz
0,15
0,10
0,05
0
Tests
M = 10
NEWTON
5°
10°
15°
i°

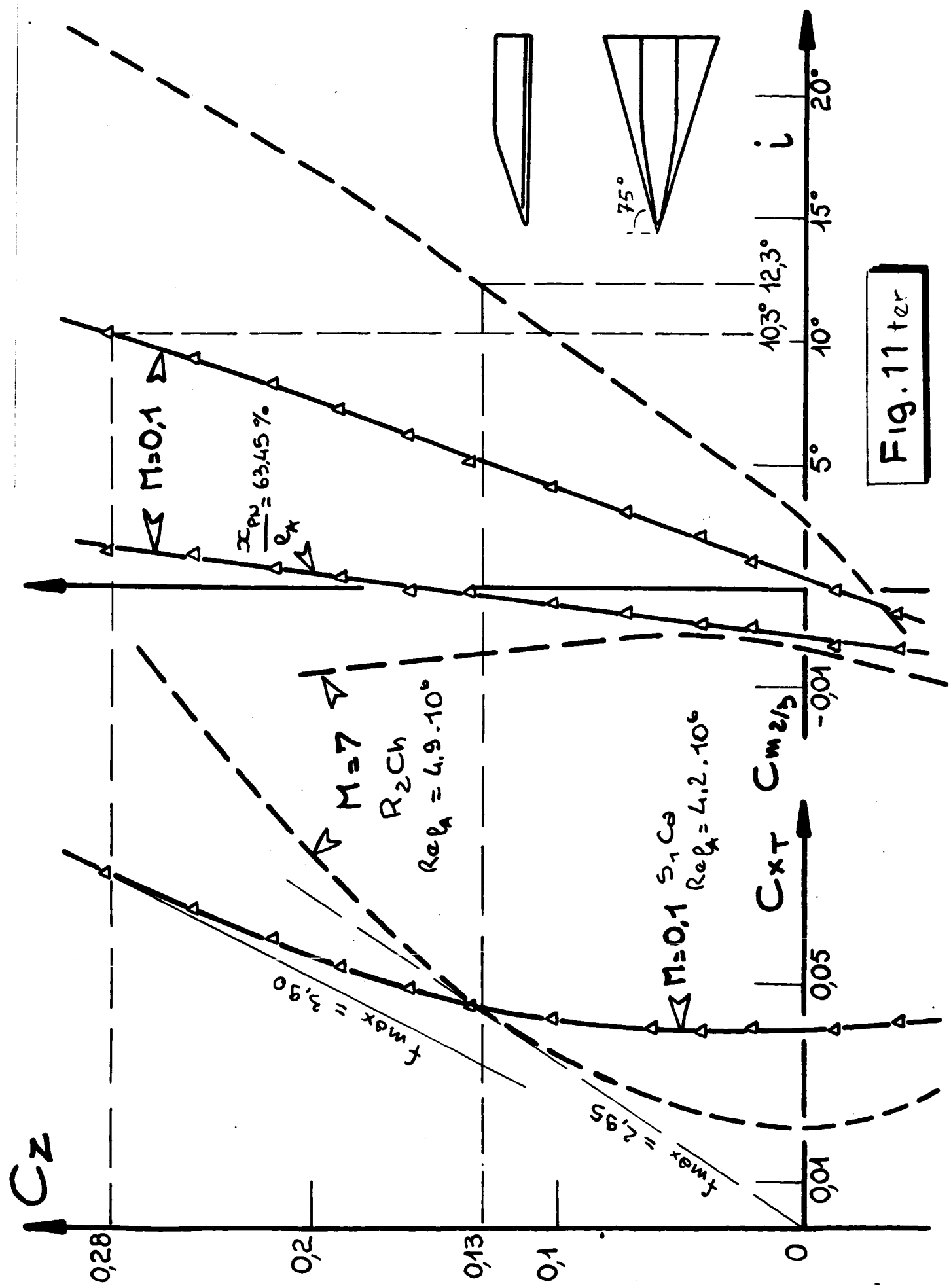
Cz
0,28
0,2
0,13
0,1
0
M=0,1
$\frac{x_{PJ}}{e_x}$ = 63,45 %
M=7
R_2Ch
$Re_{\ell_x} = 4,9.10^6$
M=0,1 S_1Ca
$Re_{\ell_x} = 4,2.10^6$
$f_{max} = 3,90$
$f_{max} = 2,95$
Cxt
$C_{m2/3}$
0,05
0,01
-0,01
i
20°
15°
12,3°
10,3°
10°
5°
75°

Fig. 11 ter

Fig. 12

Maximum fineness $(i \sim 11°)$

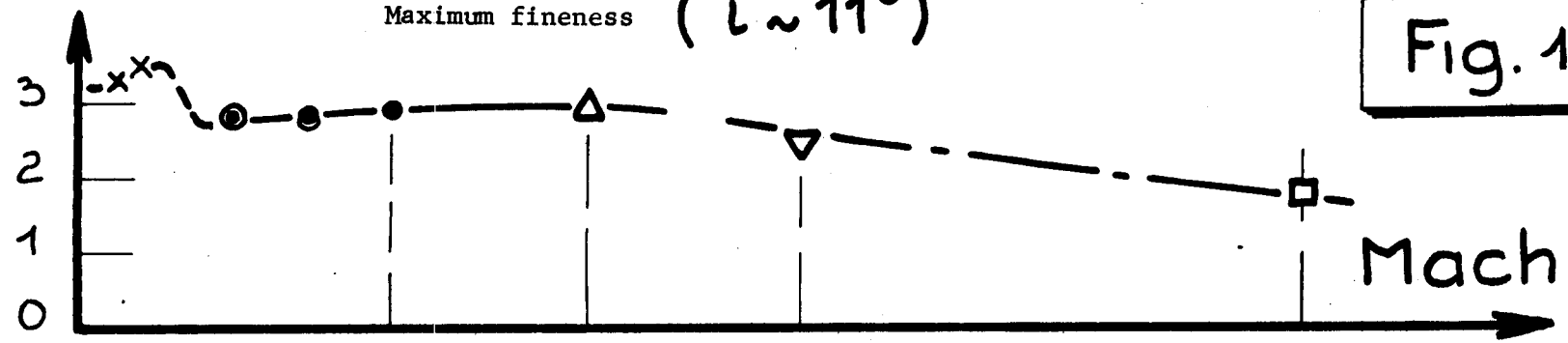

M =	4,3	7	10	17
Re_{l_A} =	$4,7.10^6$	$4,9.10^6$	$1,4.10^6$	$0,9.10^6$

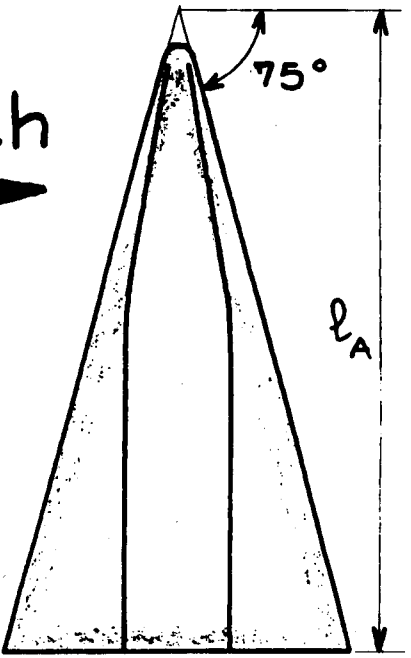

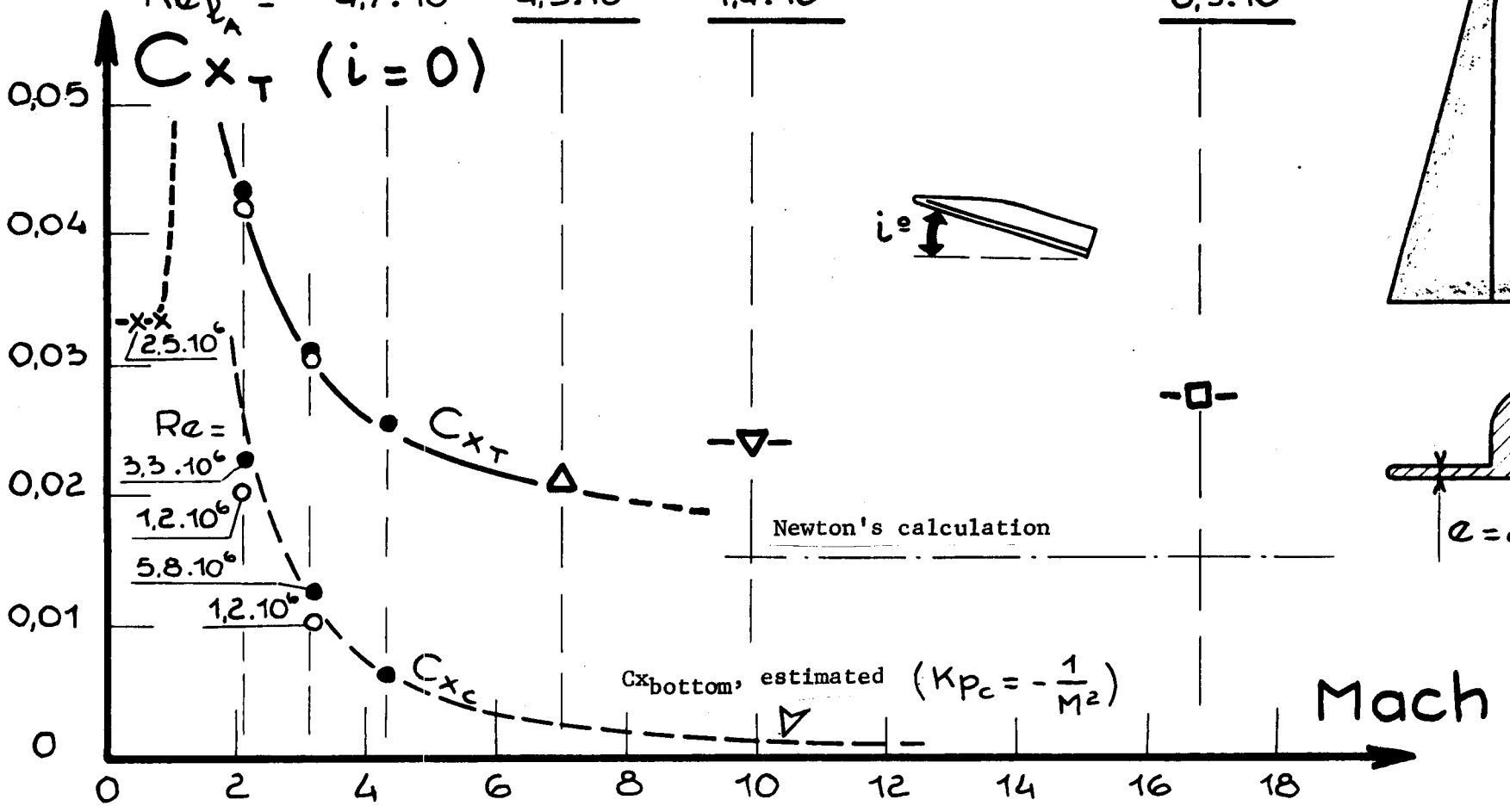

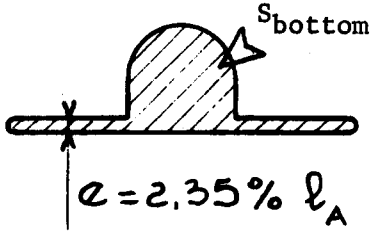

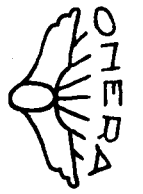

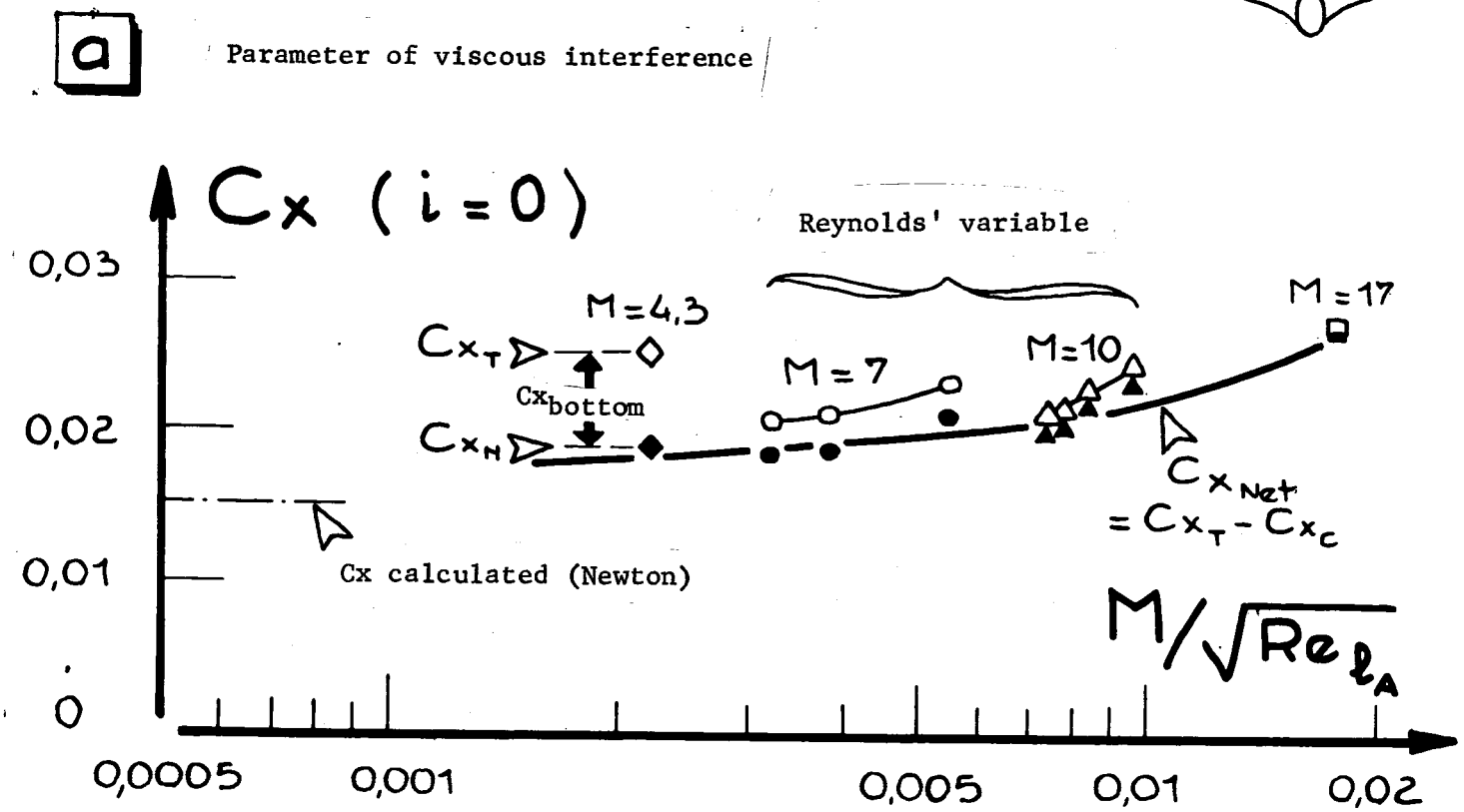
a
Parameter of viscous interference
Cx (i = 0)
Reynolds' variable
0,03
0,02
0,01
0
M = 4,3
M = 7
M = 10
M = 17
Cx_T
Cx_bottom
Cx_N
Cx_Net = Cx_T - Cx_C
Cx calculated (Newton)
M/√Re_lA
0,0005
0,001
0,005
0,01
0,02

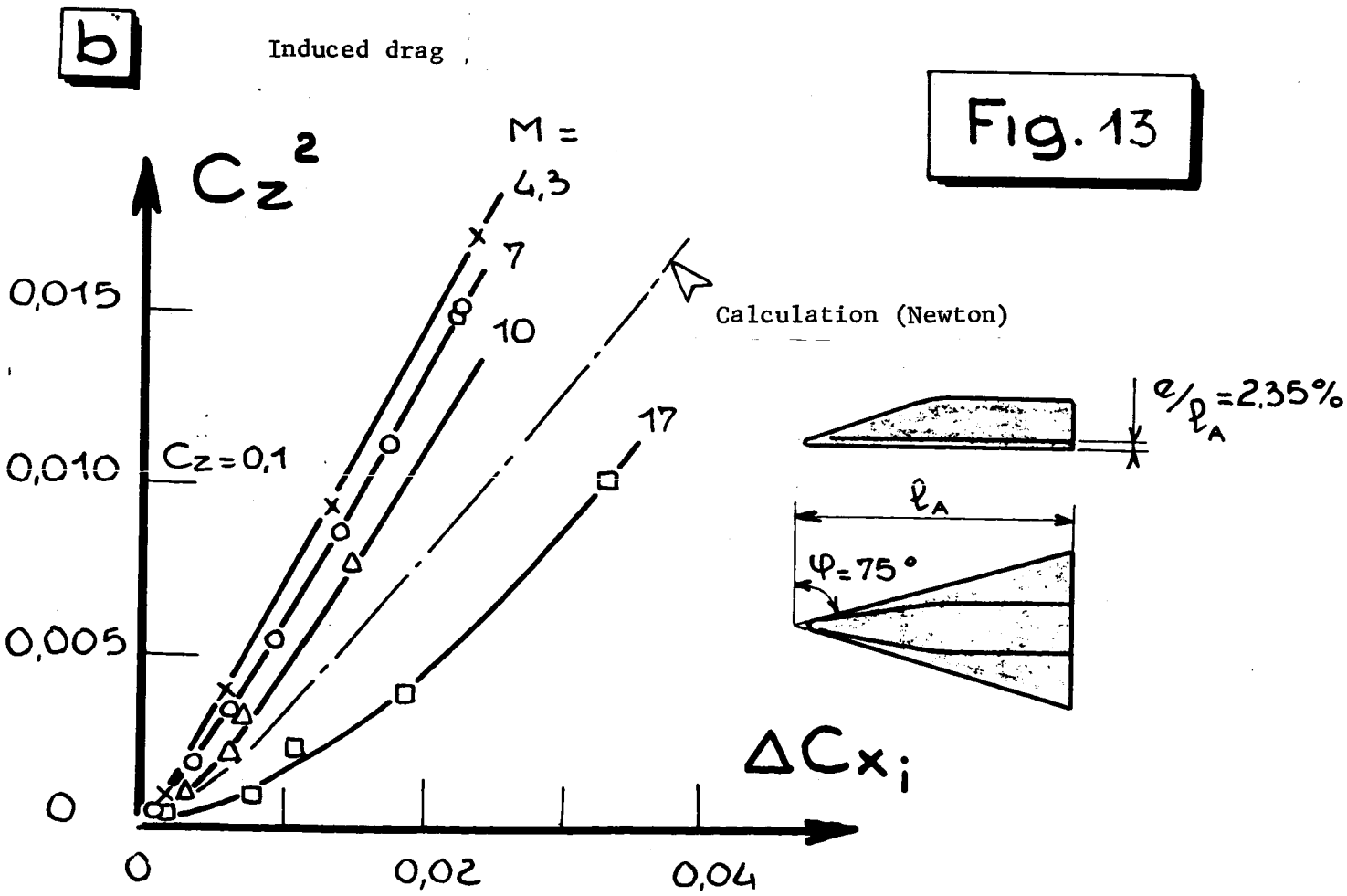
b
Induced drag
Fig. 13
Cz²
M =
4,3
7
10
17
0,015
0,010
0,005
0
Cz = 0,1
Calculation (Newton)
e/l_A = 2,35%
l_A
φ = 75°
ΔCx_i
0
0,02
0,04

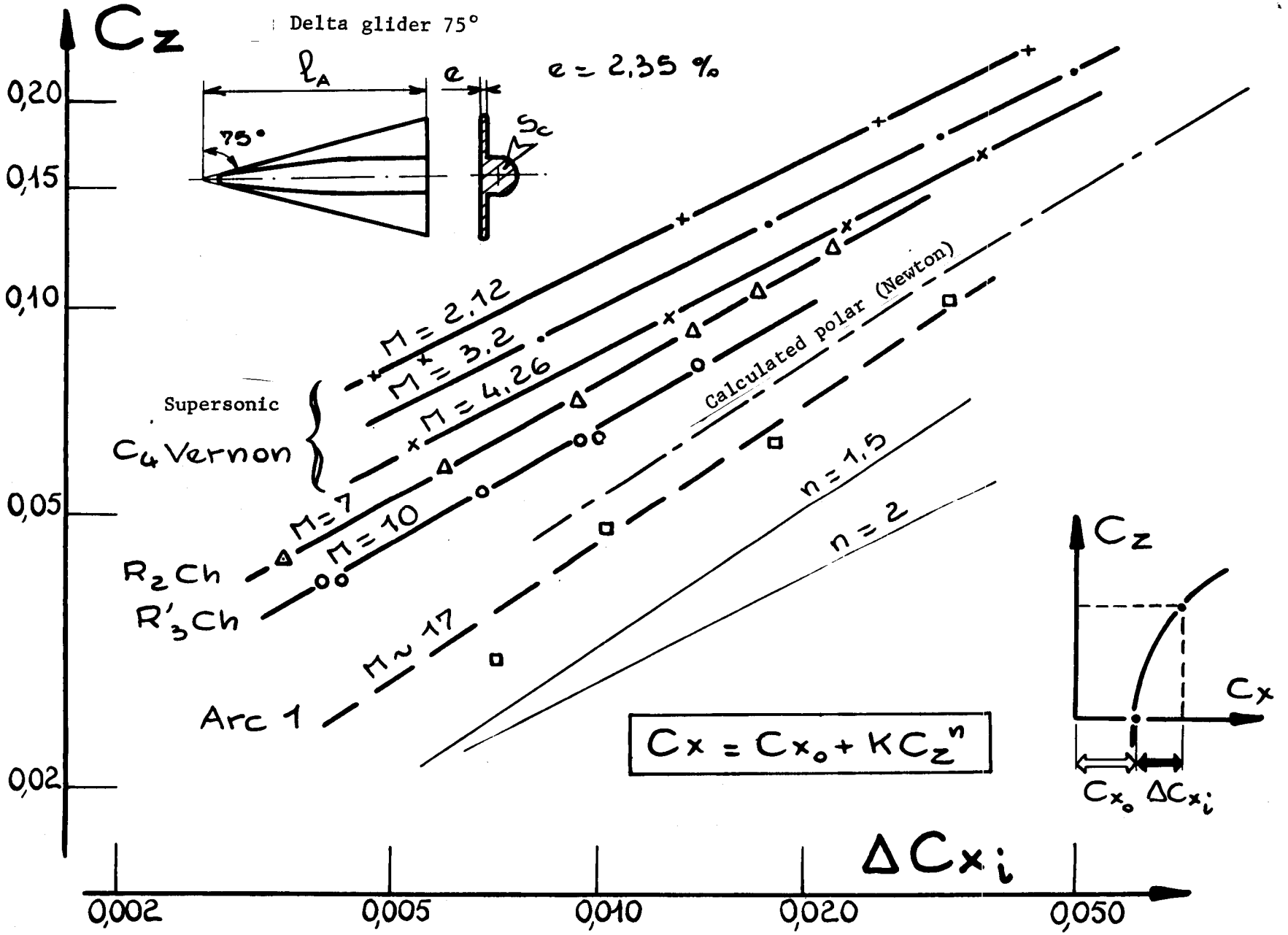

Fig. 13 Induced resistance

Longitudinal stability

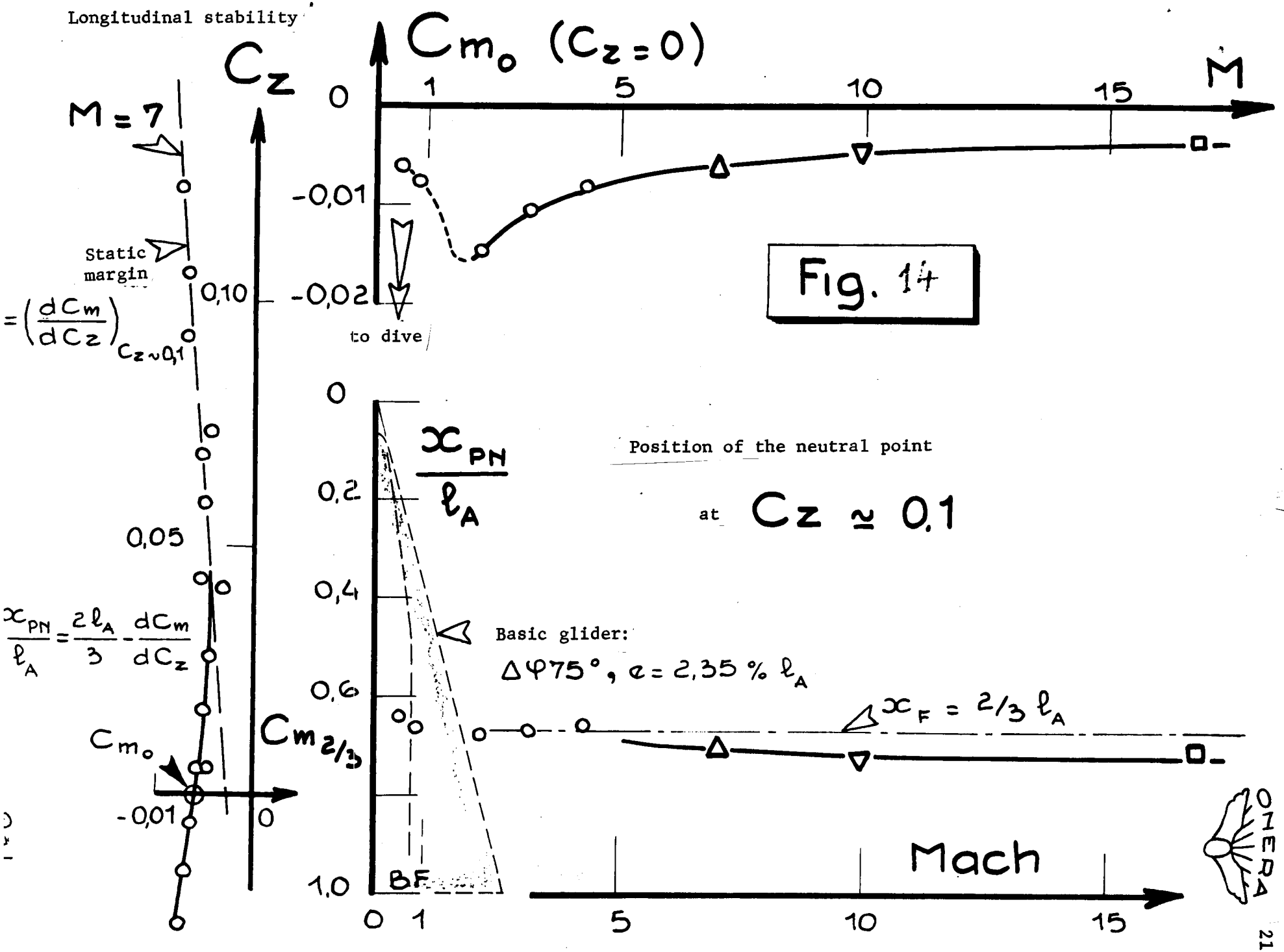

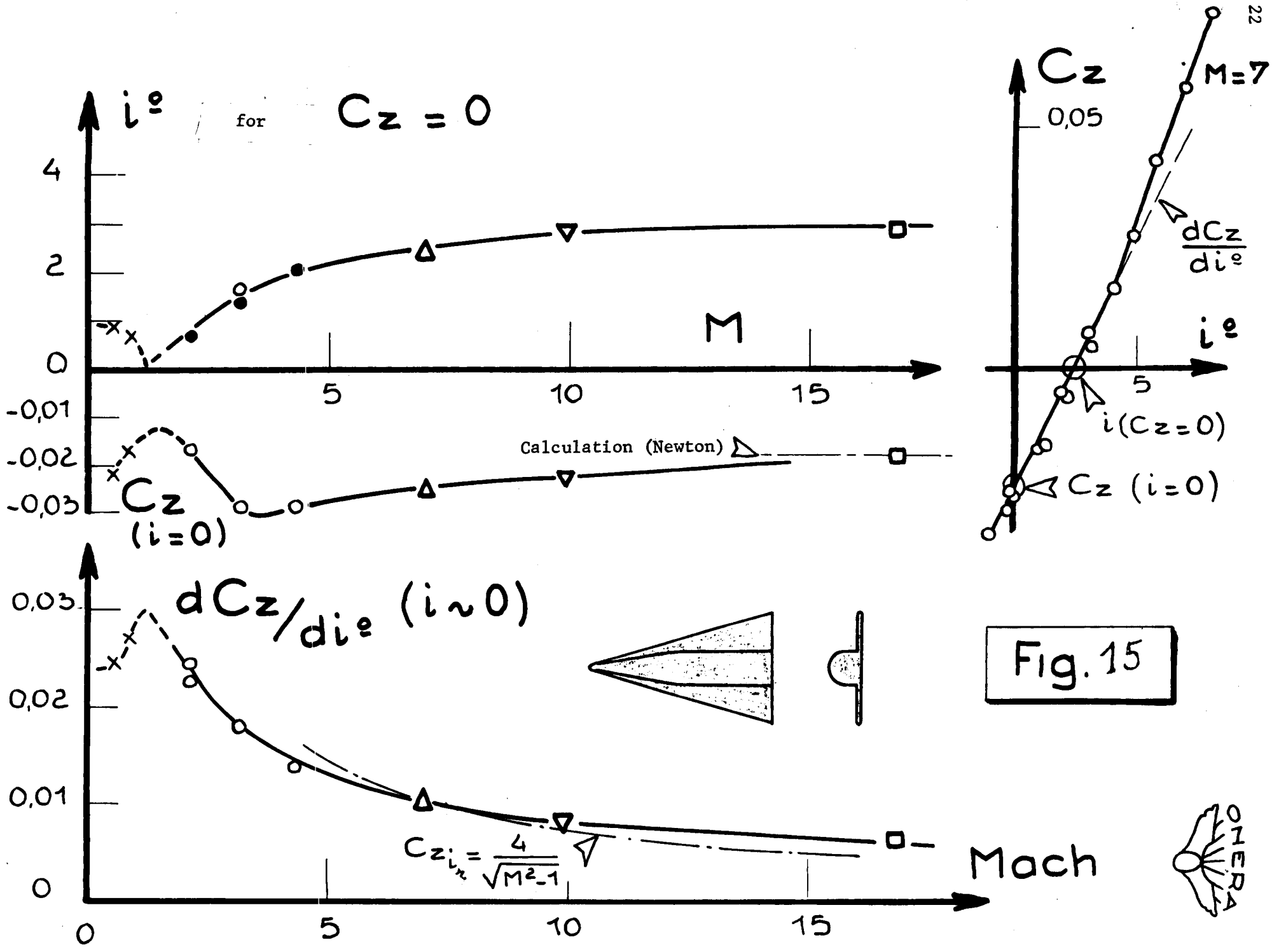
i° for Cz = 0
4
2
0
-0,01
-0,02
-0,03
5
10
15
M
Calculation (Newton)
Cz (i=0)
Cz
0,05
M=7
dCz/di°
i°
5
i(Cz=0)
Cz (i=0)
dCz/di° (i~0)
0,03
0,02
0,01
0
Cz i∞ = 4/√(M²-1)
Mach
ONERA

Fig. 15

Glider, Δ75° at high incidences

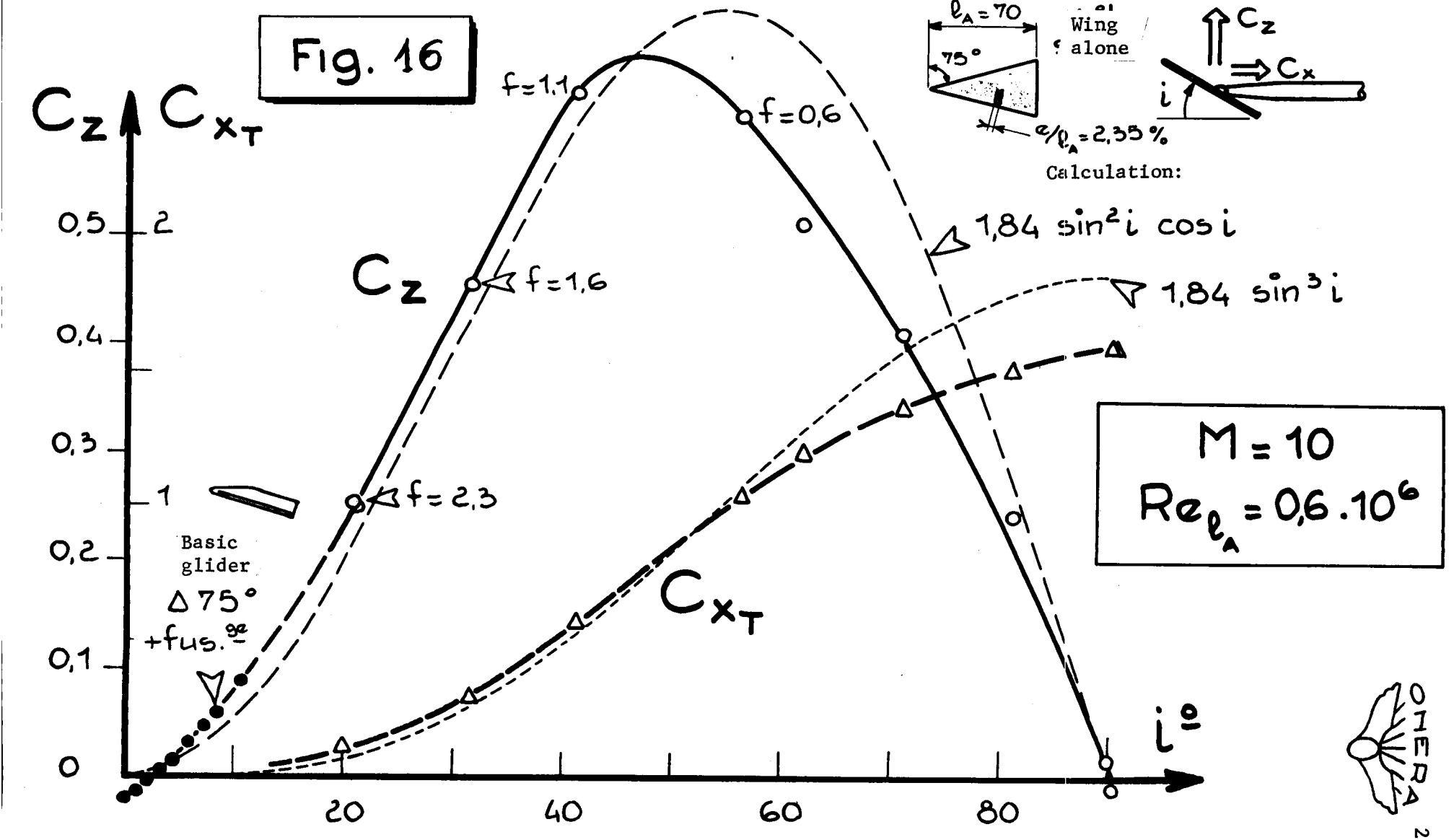

Effect of the thickness of the wing

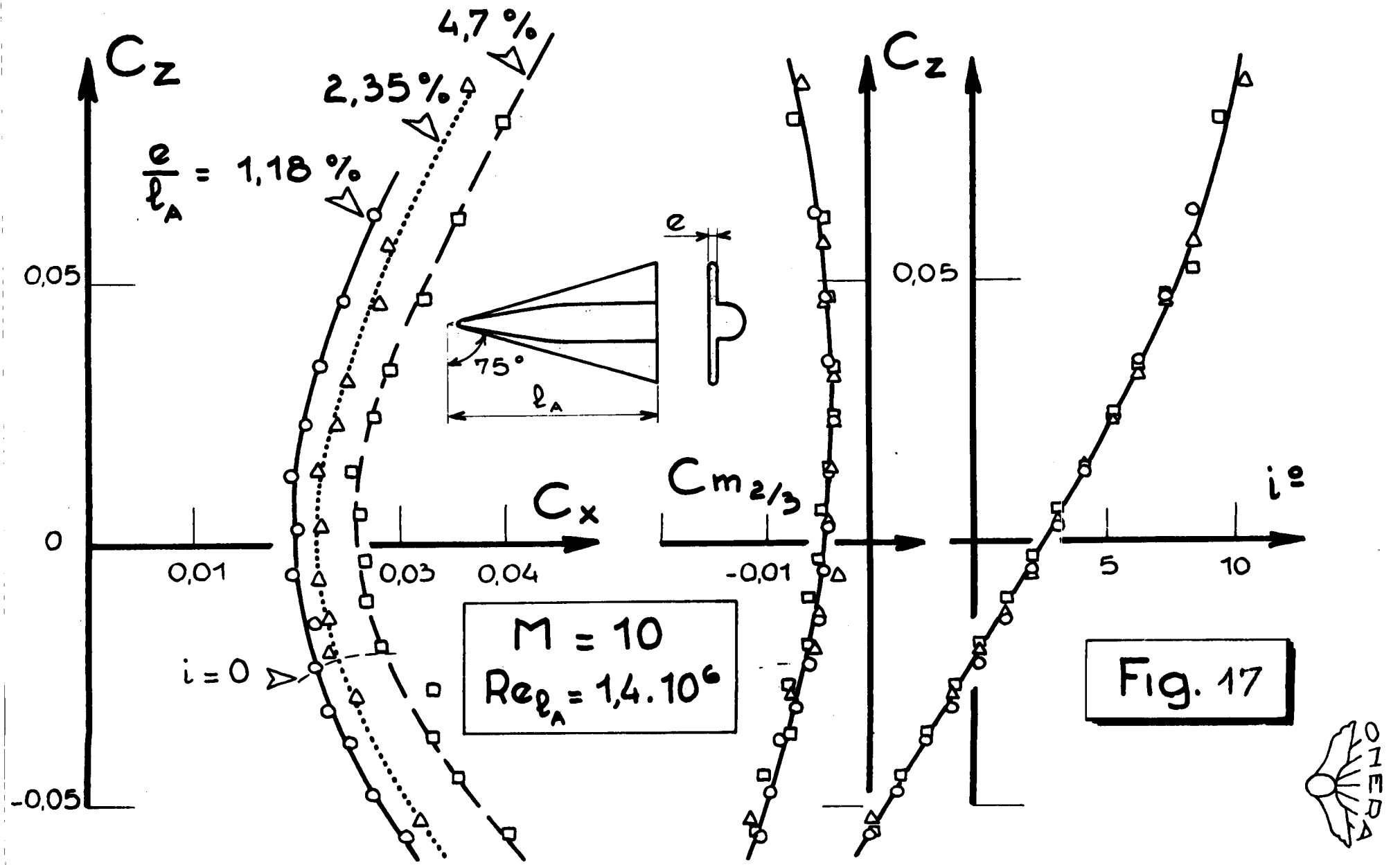

Fig. 17

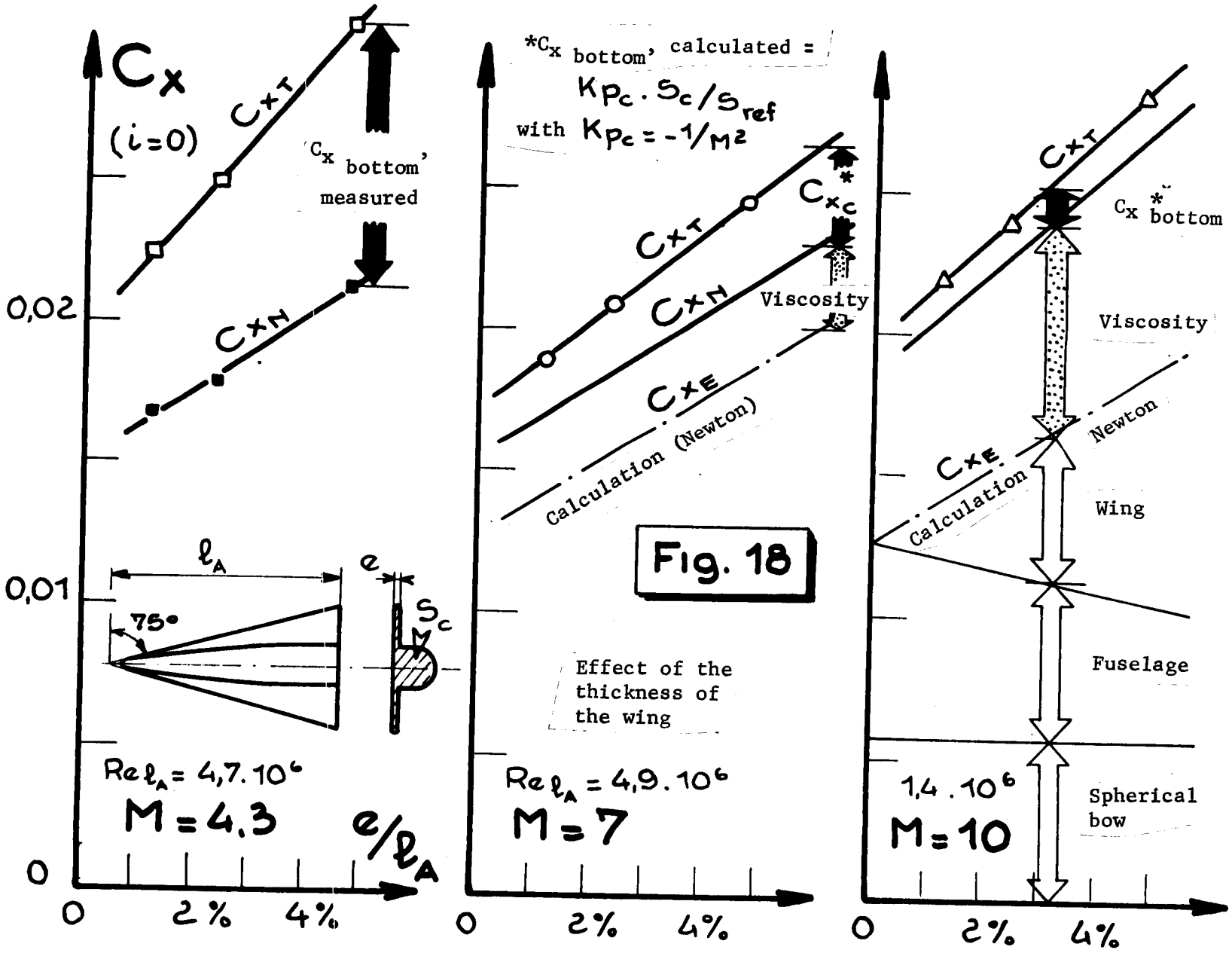
Cx
(i=0)
Cx bottom' measured
Cx T
Cx N
0,02
0,01
0
ℓ_A
e
75°
S_c
$Re\ell_A = 4,7.10^6$
M = 4.3
e/ℓ_A
0
2%
4%
*Cx bottom' calculated =
$Kp_c . S_c/S_{ref}$
with $Kp_c = -1/M^2$
Cx T
Cx N
Cx E
Calculation (Newton)
Cx c*
Viscosity
Effect of the thickness of the wing
$Re\ell_A = 4,9.10^6$
M = 7
Cx T
Cx N
Cx E
Calculation
Cx bottom*
Viscosity
Newton
Wing
Fuselage
Spherical bow
$1,4.10^6$
M = 10

Fig. 18

Effect of the sweep
(identical surface)

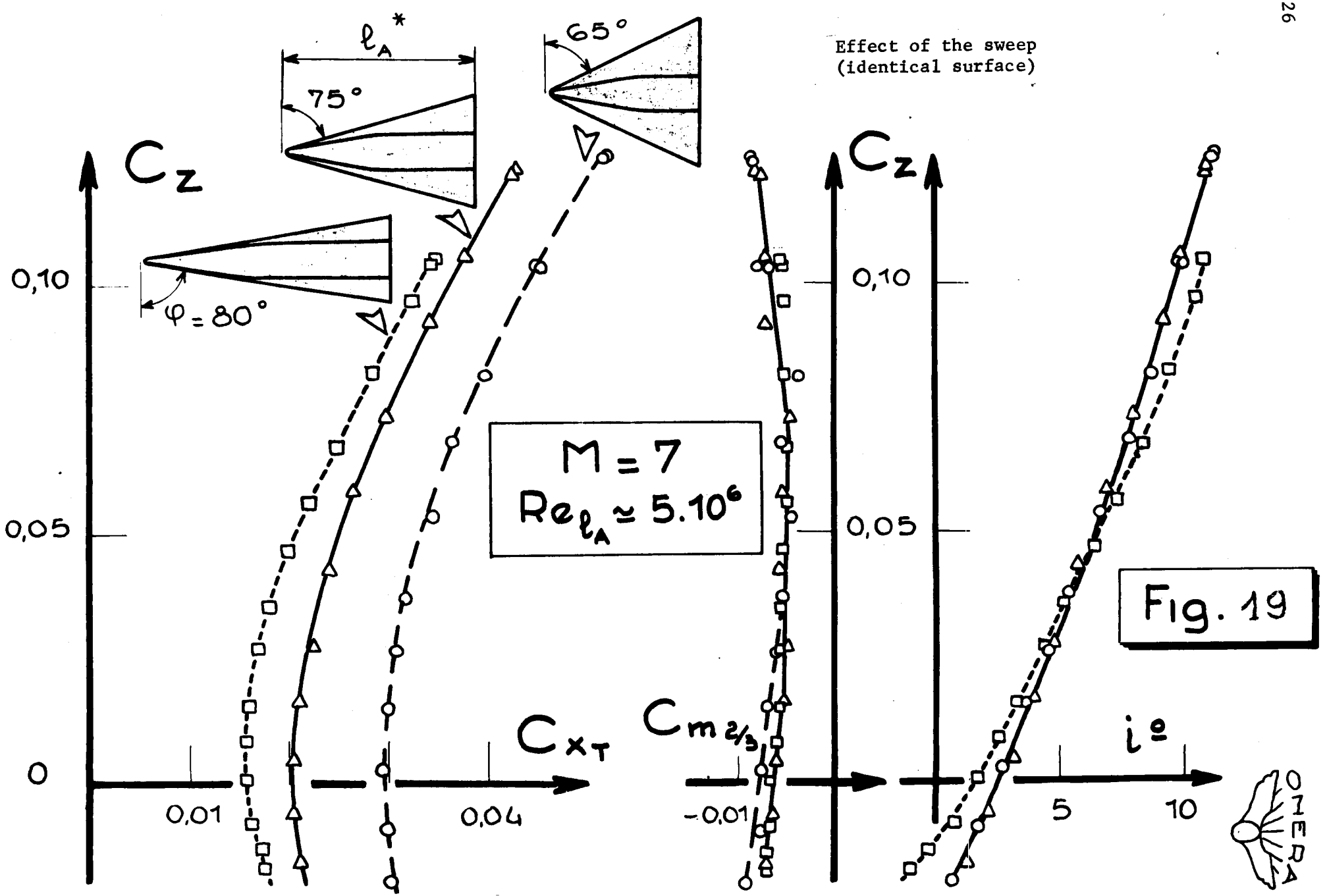

Fig. 19

*l_A varies with φ: same ogive of the fuselage; same absolute thickness of the flat wing (2 5% .075)

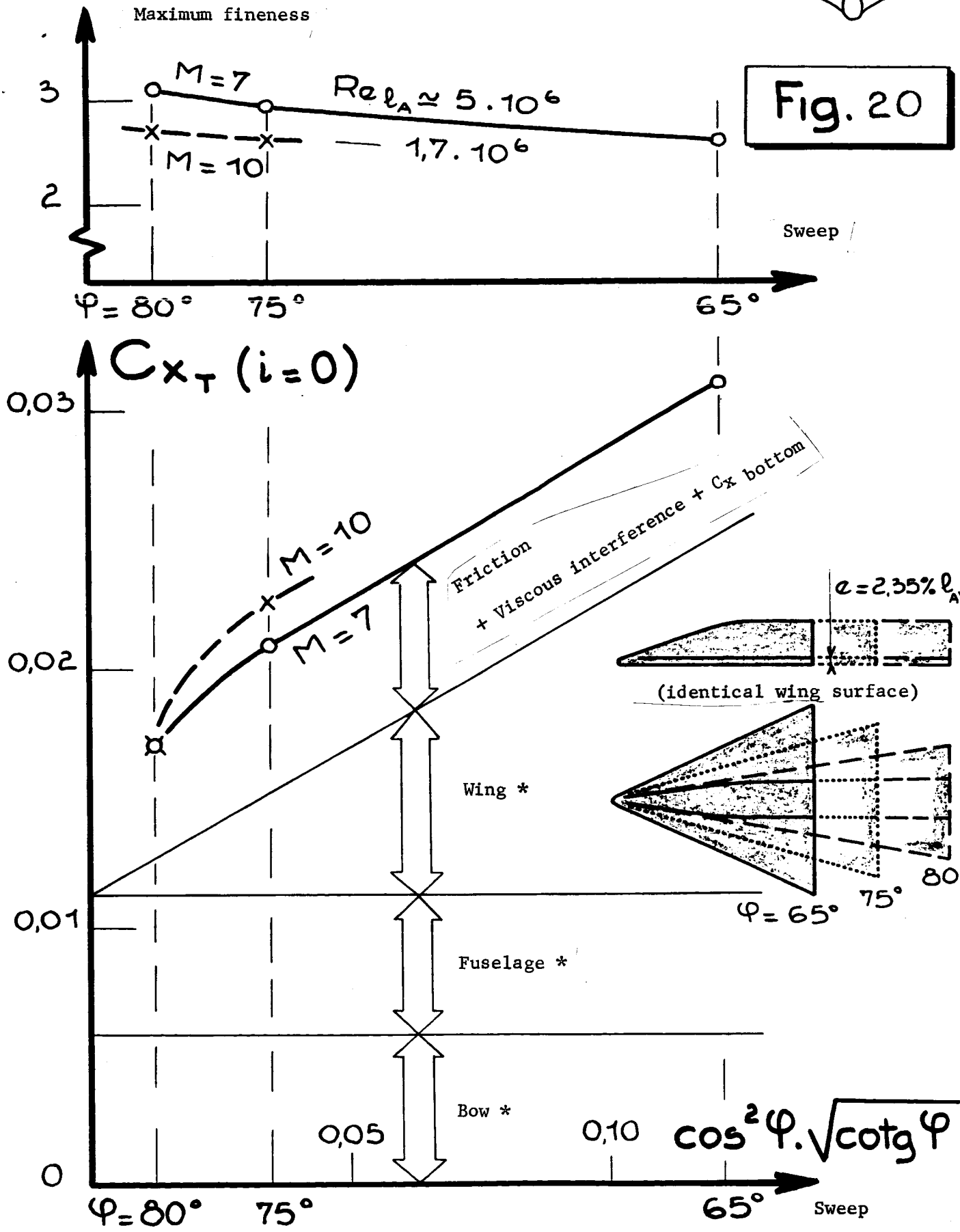
Maximum fineness
3
2
M=7
$Re\,l_A \simeq 5.10^6$
M=10
1,7.10⁶
Sweep
φ=80°
75°
65°
C_{x_T} (i=0)
0,03
0,02
0,01
0
M=10
M=7
Friction
+ Viscous interference + Cx bottom
Wing *
Fuselage *
Bow *
0,05
0,10
$\cos^2\varphi.\sqrt{\cot g\,\varphi}$
e=2,35% l_{A75}
(identical wing surface)
φ=65°
75°
80°
φ=80°
75°
65°
Sweep
*Newton's calculation

Fig. 20

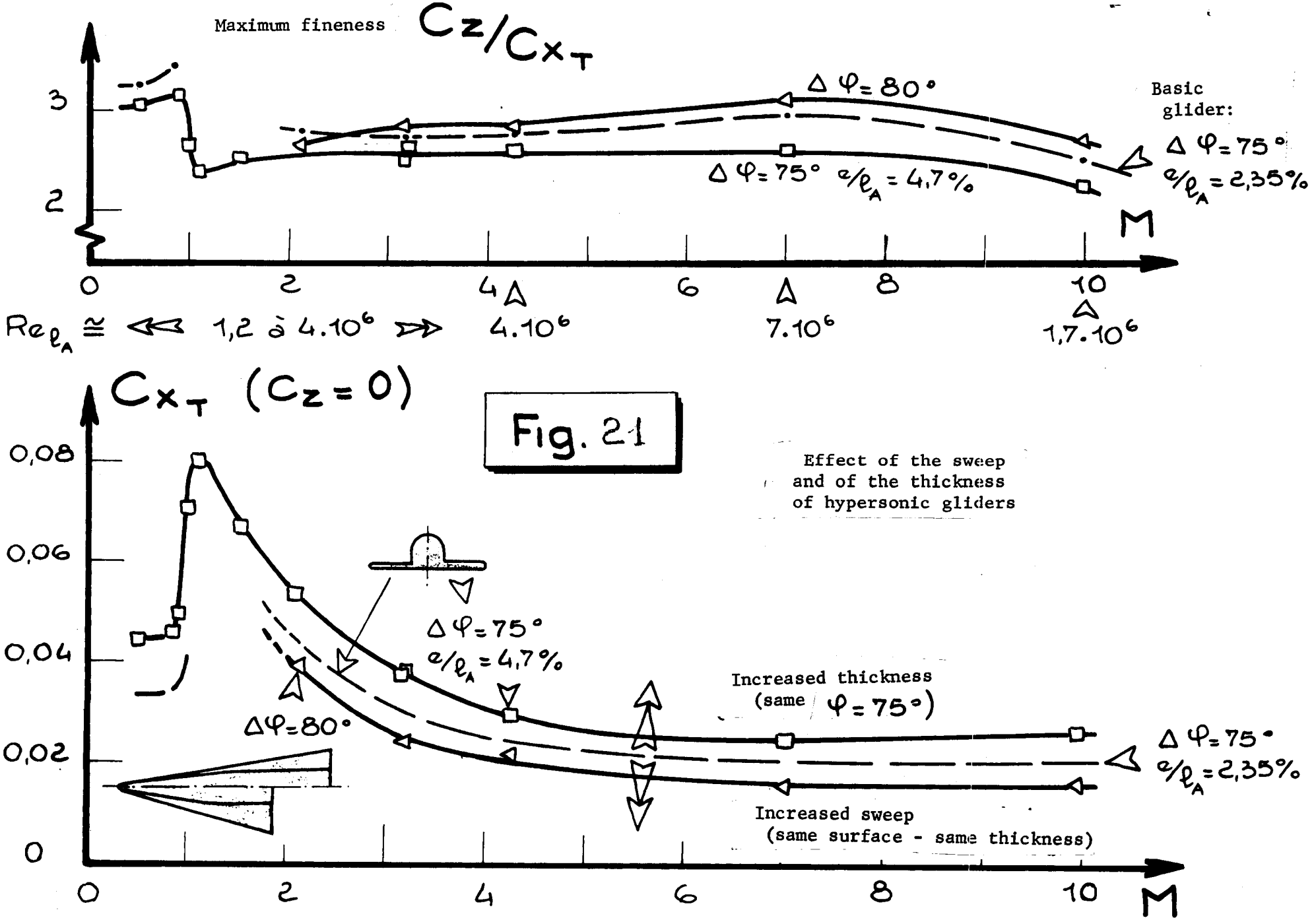

Fig. 21

Effect of the sweep and of the thickness of hypersonic gliders

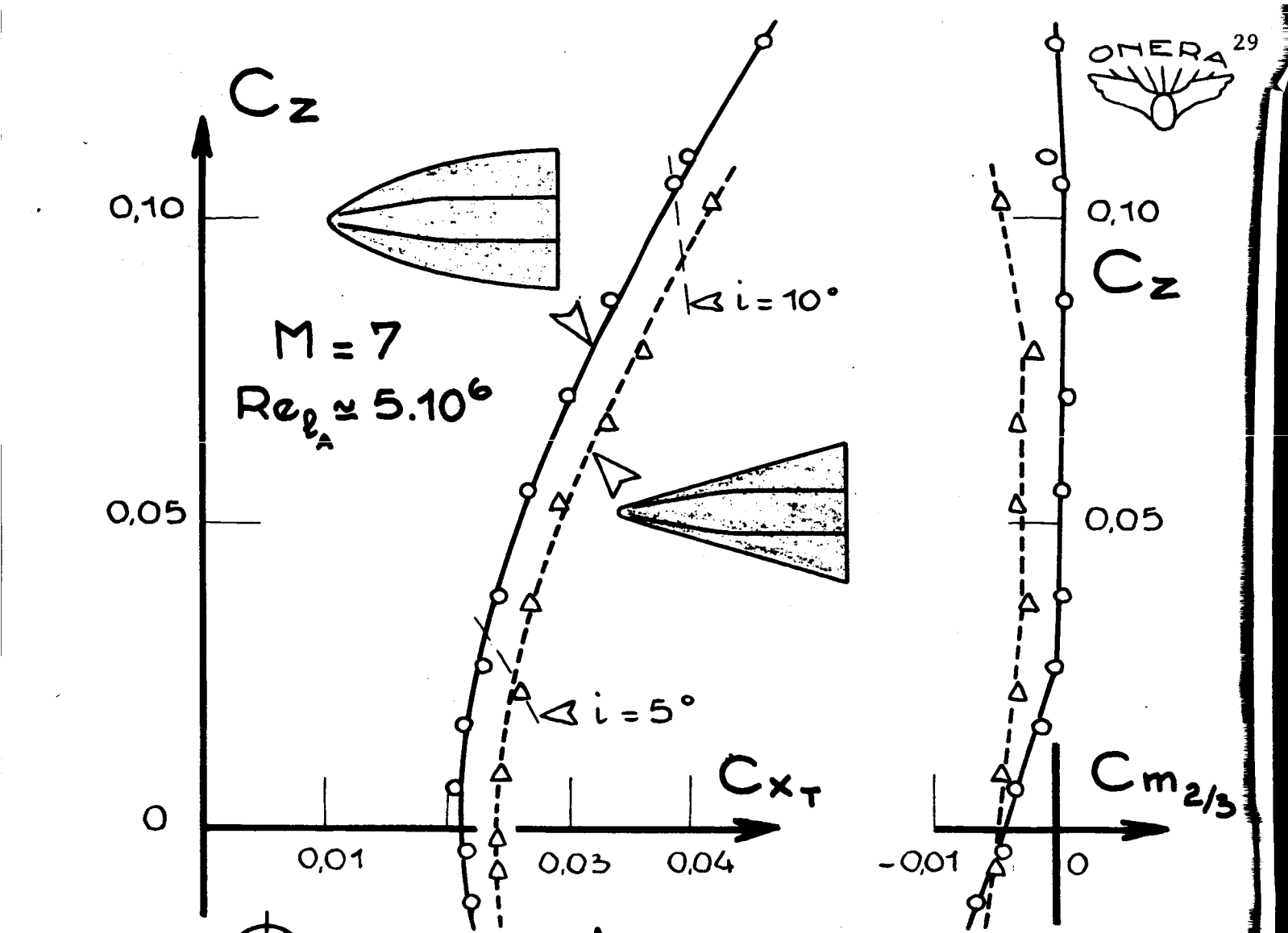
C_z
0,10
0,05
0
M = 7
$Re_{l_A} \simeq 5.10^6$
i = 10°
i = 5°
C_{x_T}
0,01
0,03
0,04
0,10
C_z
0,05
$C_{m_{2/3}}$
-0,01
0

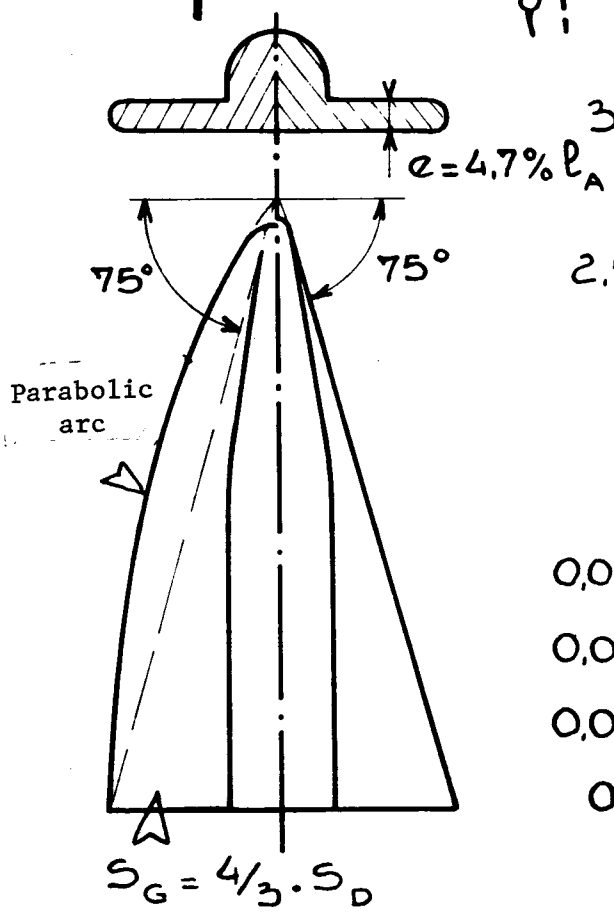
e = 4,7% l_A
75°
75°
Parabolic arc
$S_G = 4/3 . S_D$

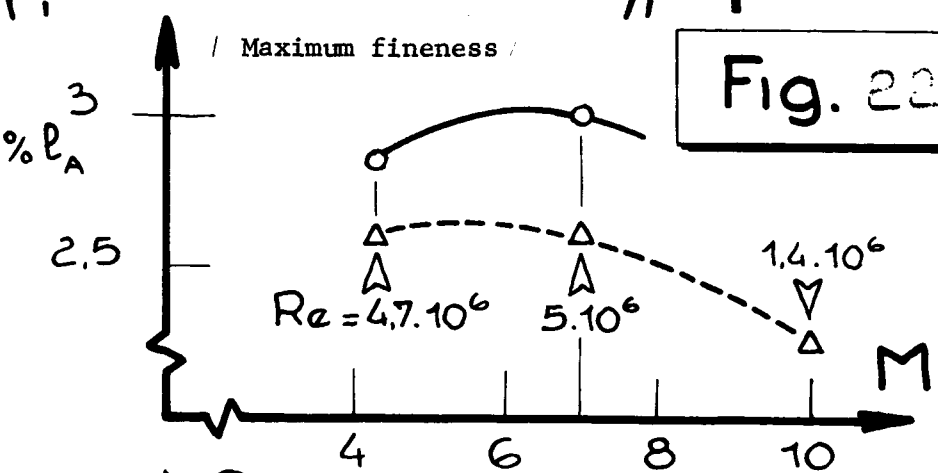
/ Maximum fineness /
3
2,5
$Re = 4,7.10^6$
5.10^6
$1,4.10^6$
M
4
6
8
10

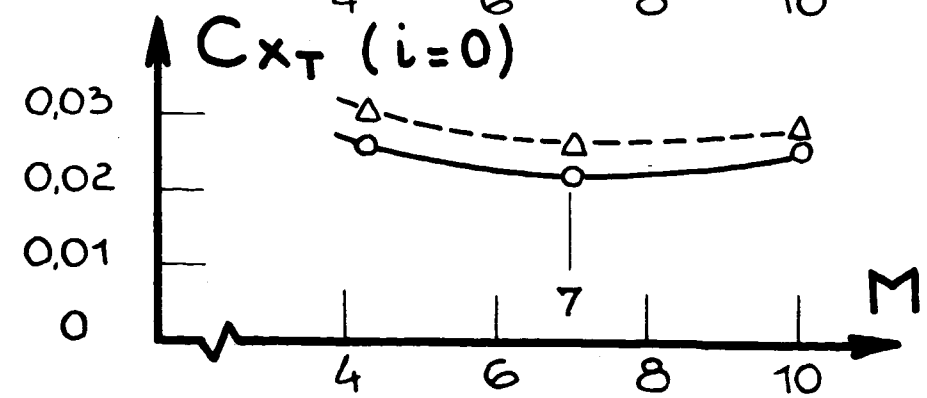
C_{x_T} (i=0)
0,03
0,02
0,01
0
7
M
4
6
8
10

Fig. 22

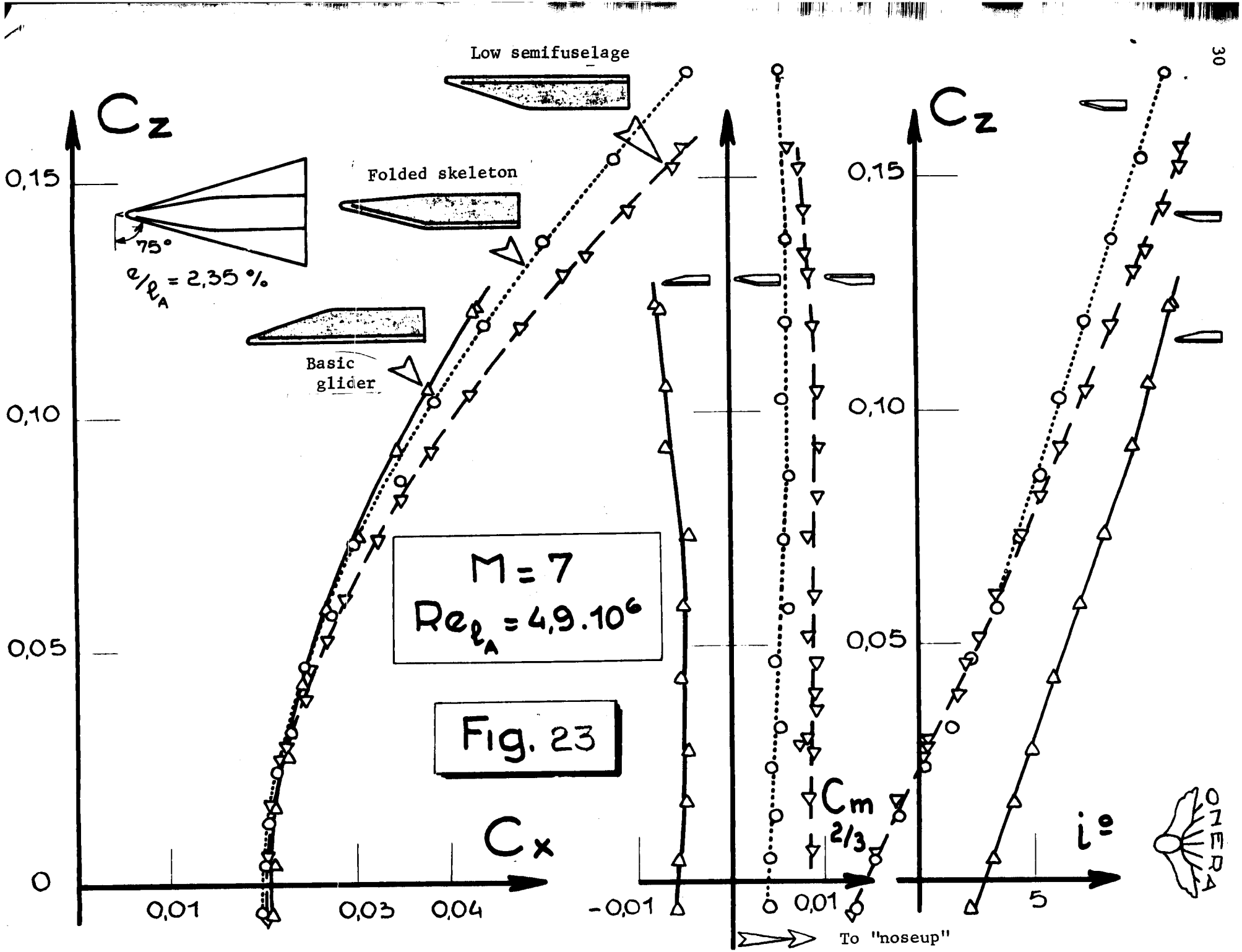
Low semifuselage
Folded skeleton
Basic glider
75°
e/ℓA = 2,35 %
Cz
0,15
0,10
0,05
0
0,01
0,03
0,04
Cx
M = 7
ReℓA = 4,9.10⁶
Fig. 23
-0,01
0
0,01
Cm 2/3
To "noseup"
Cz
0,15
0,10
0,05
5
i°
ONERA

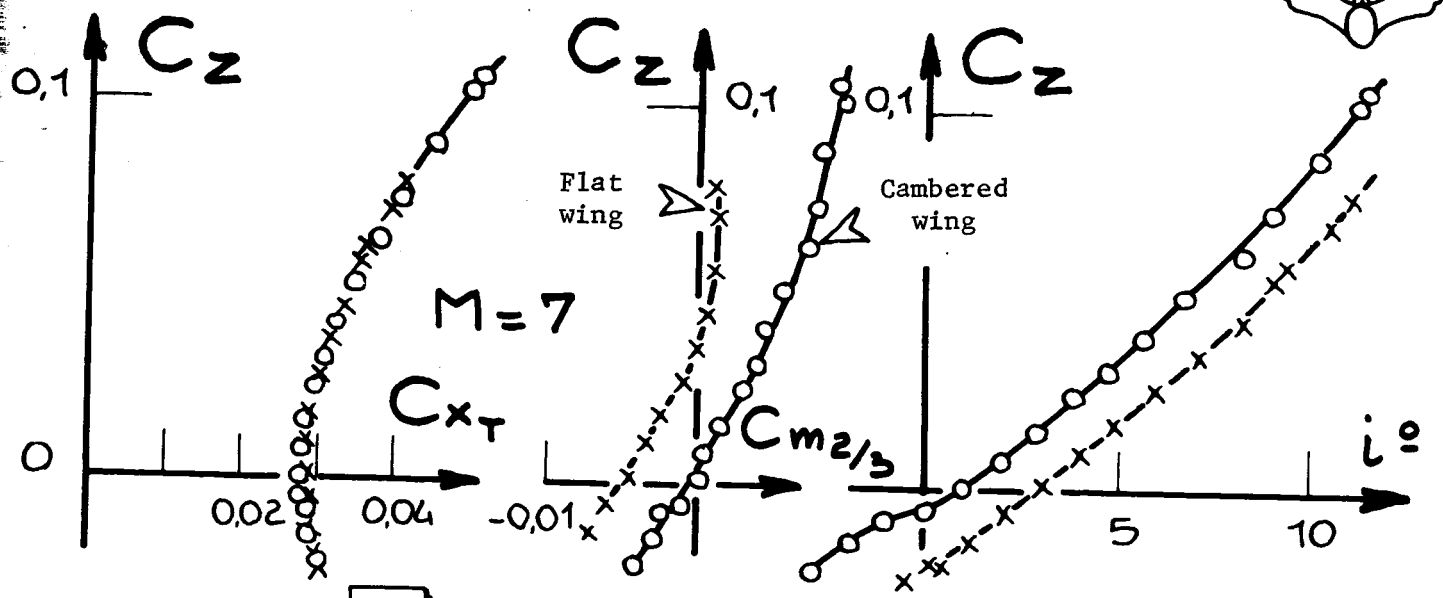

a Effect of cambering

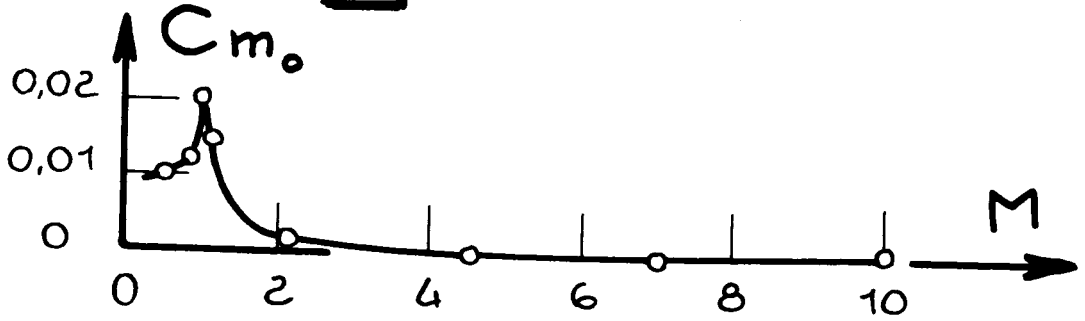

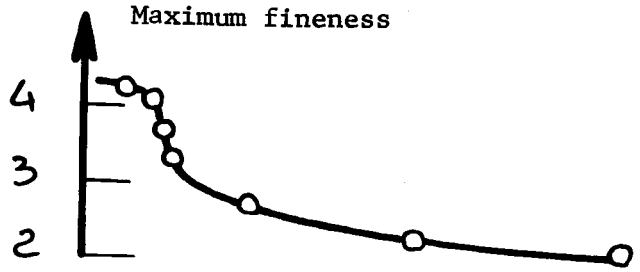

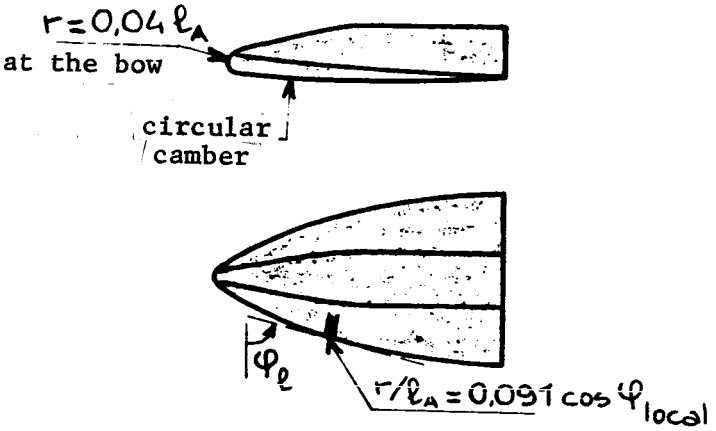

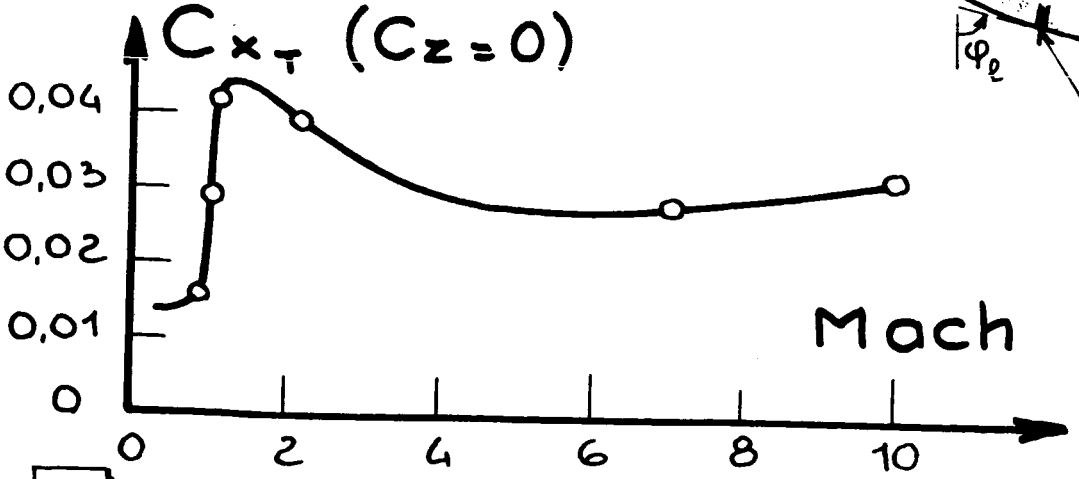

b Evolutive cambered Gothic wing of 75°

Fig. 24

ONERA

Wind tunnel R'_3 at Chalais

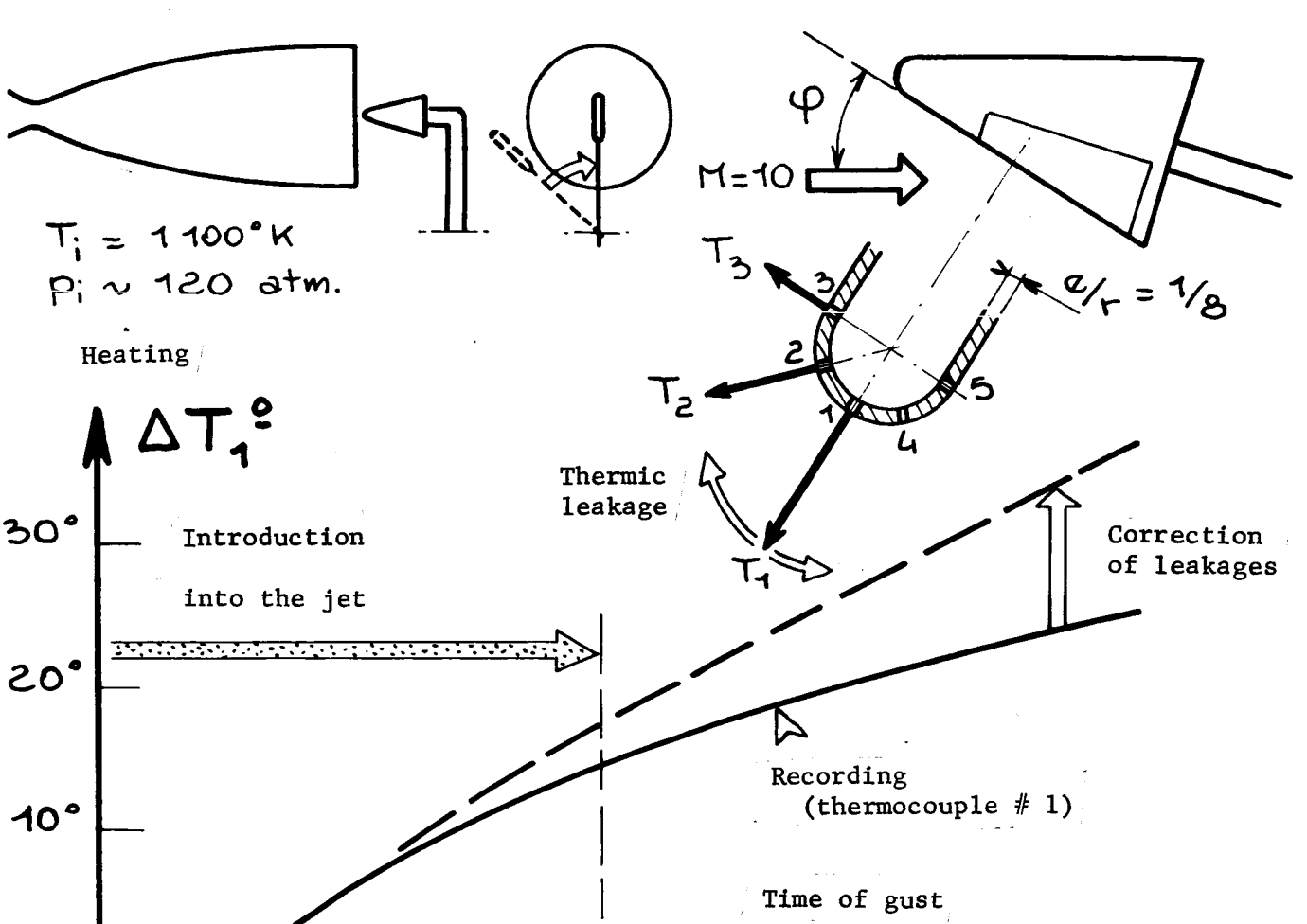

Flow with sweep / Flow at $\varphi = 0$

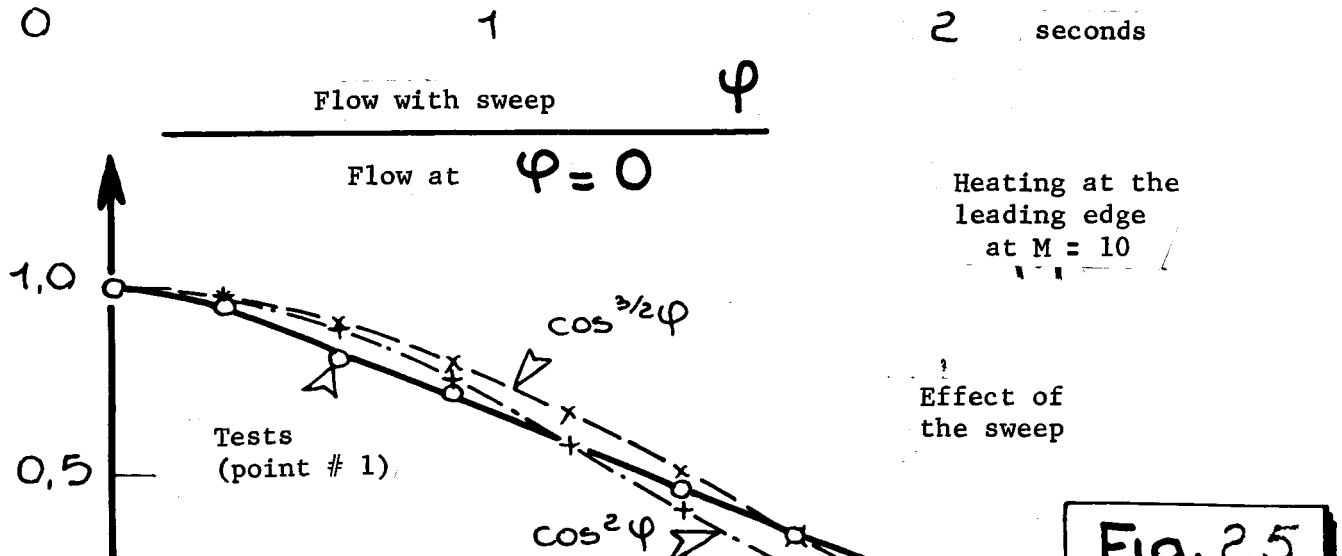

Fig. 25

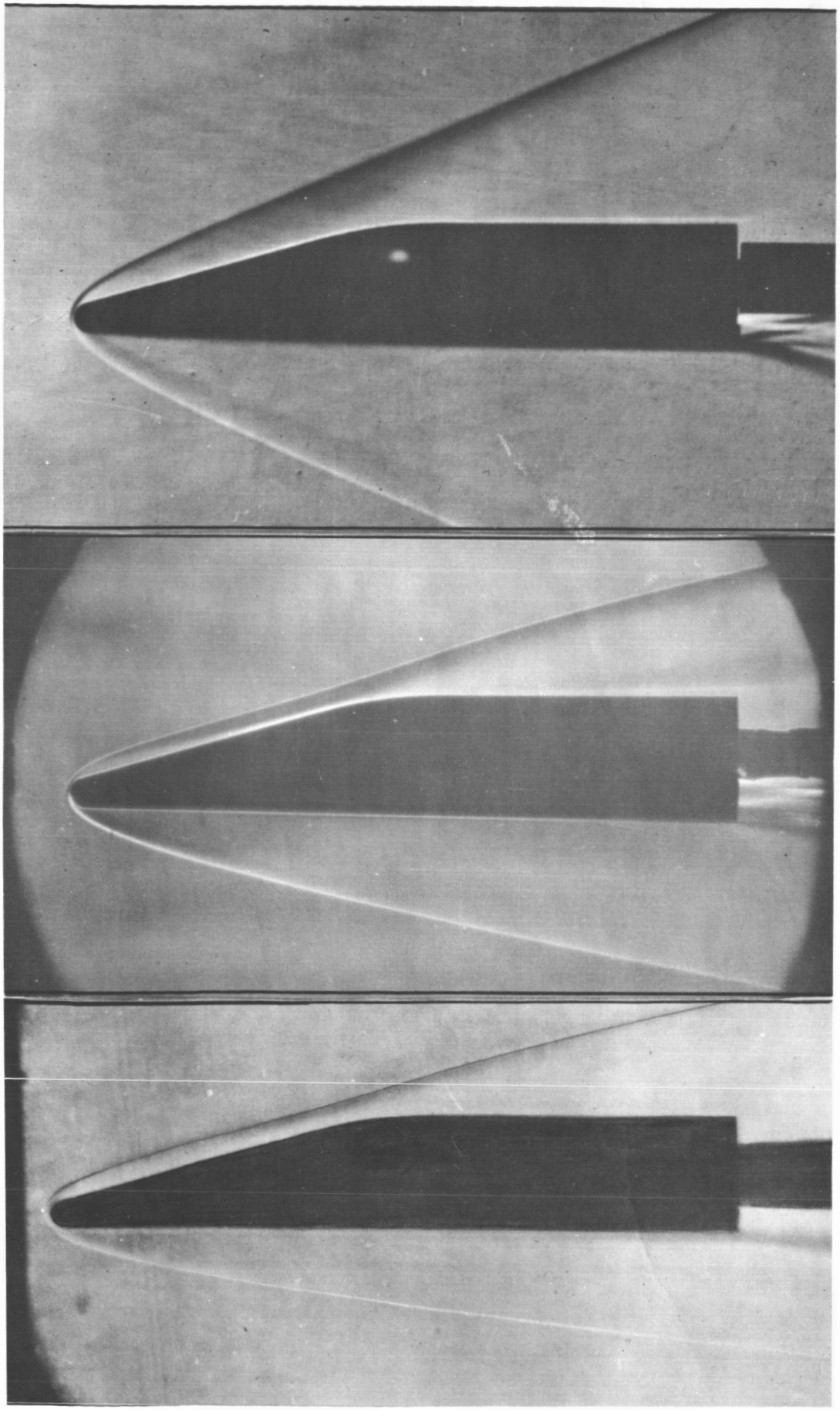

Fig. 26

Basic glider, Δ of 75° at i = 0

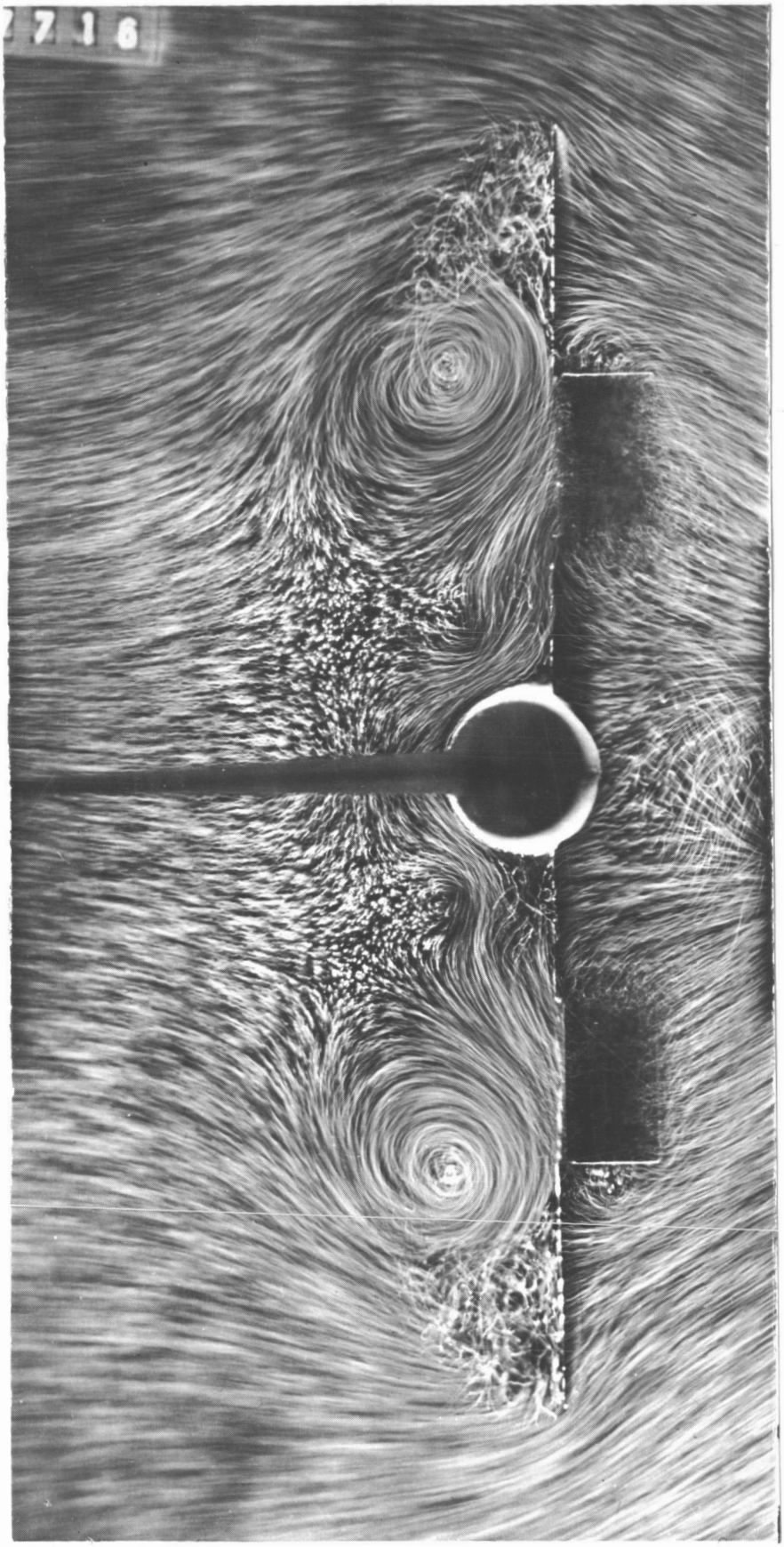
7716